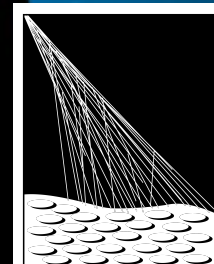


Radio detection of cosmic rays with the Auger Engineering Radio Array



Florian Gâté for the Pierre Auger Collaboration



PIERRE
AUGER
OBSERVATORY

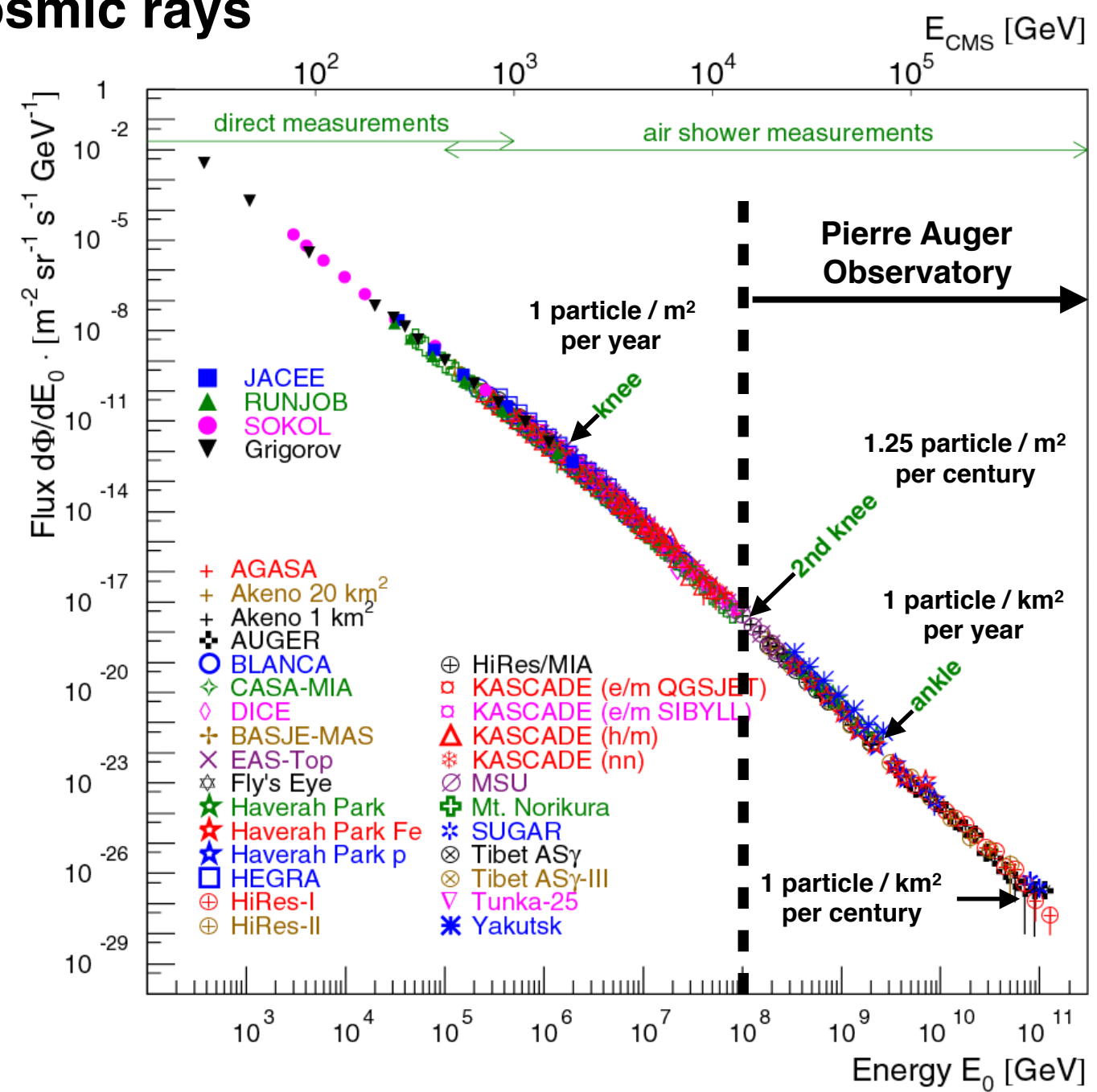
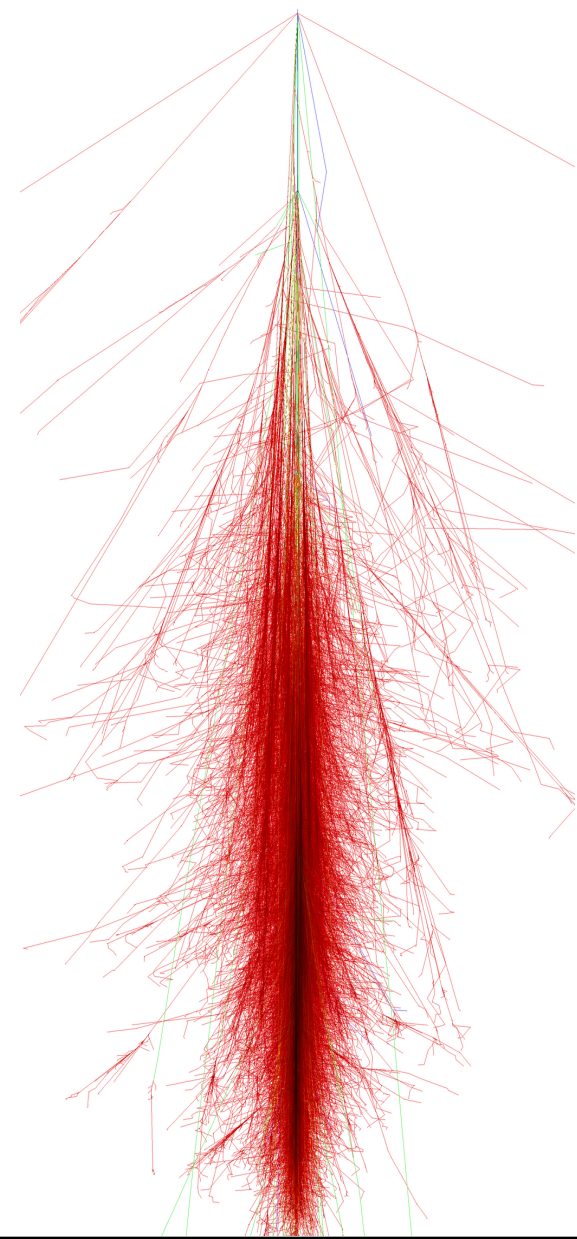
The Pierre Auger Observatory

- Located in Malargüe, Argentina
- world's largest cosmic ray detector (3000 km²)



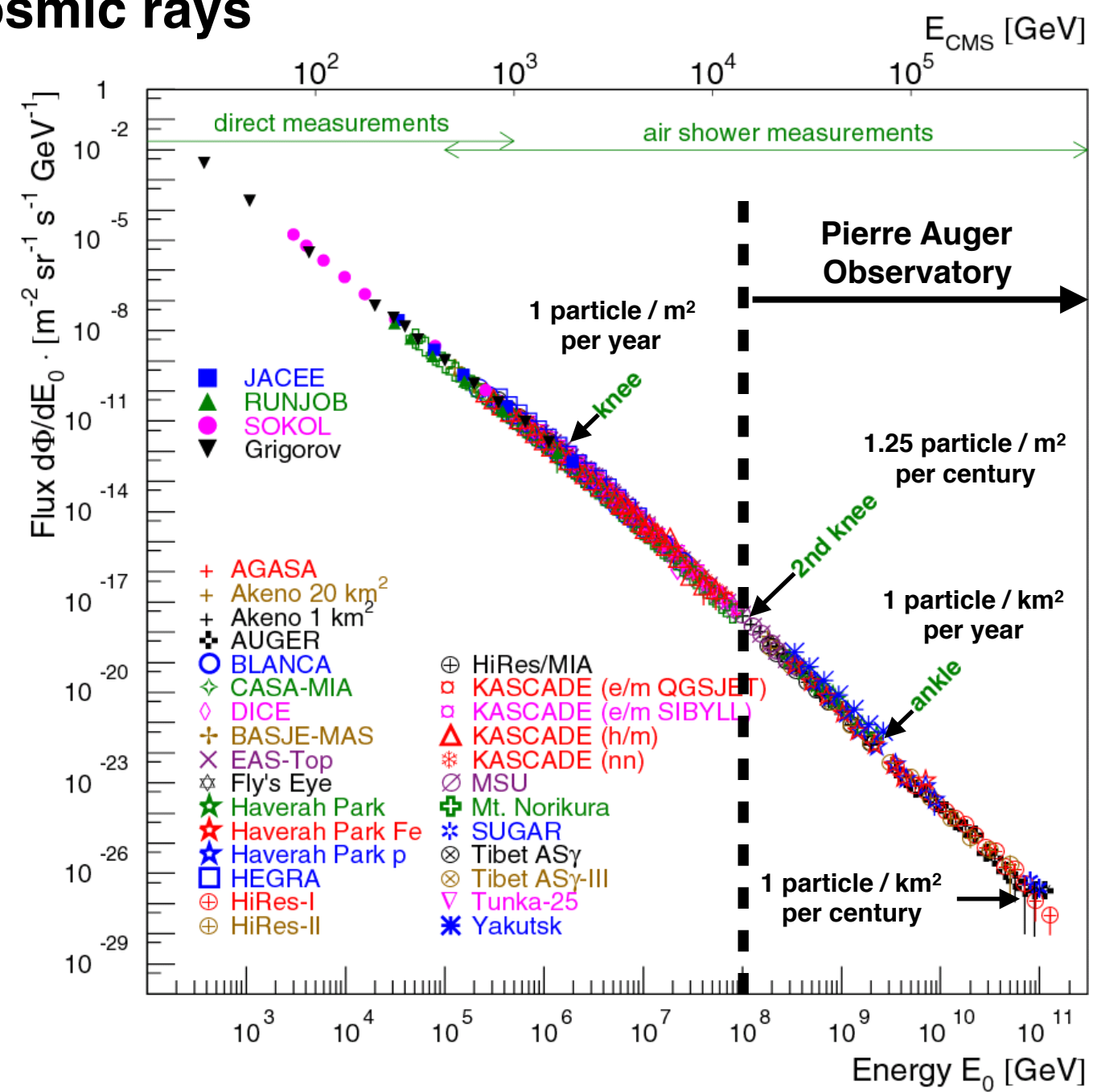
The Pierre Auger Observatory

- Located in Malargüe, Argentina
- world's largest cosmic ray detector (3000 km^2)
- detection of air showers induced by cosmic rays
 $E > 10^{17} \text{ eV}$



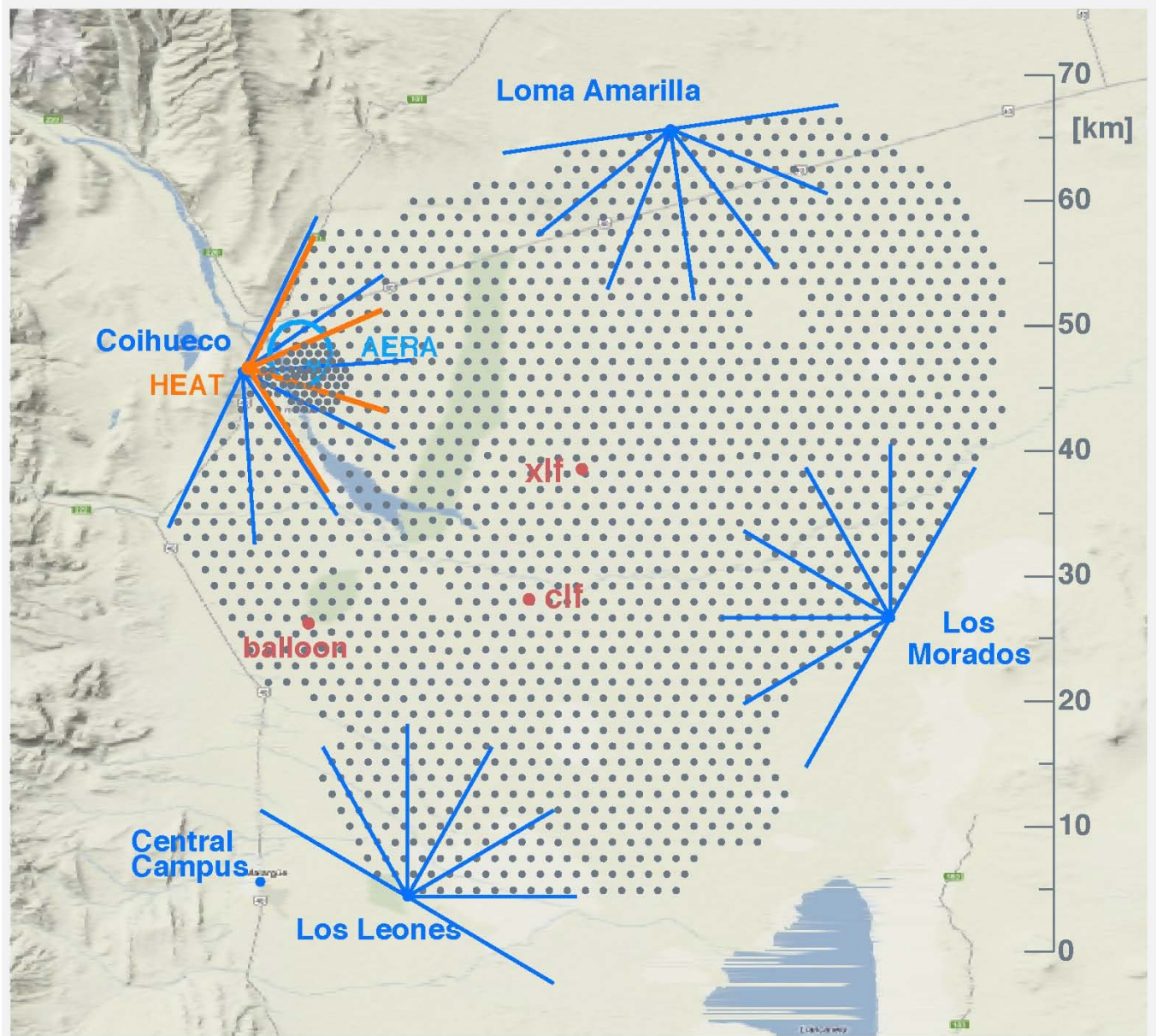
The Pierre Auger Observatory

- Located in Malargüe, Argentina
- world's largest cosmic ray detector (3000 km^2)
- detection of air showers induced by cosmic rays
 $E > 10^{17} \text{ eV}$
- physics goals
 - sources
 - acceleration mechanisms
 - origin of the cut-off
 - mass composition



The Pierre Auger Observatory

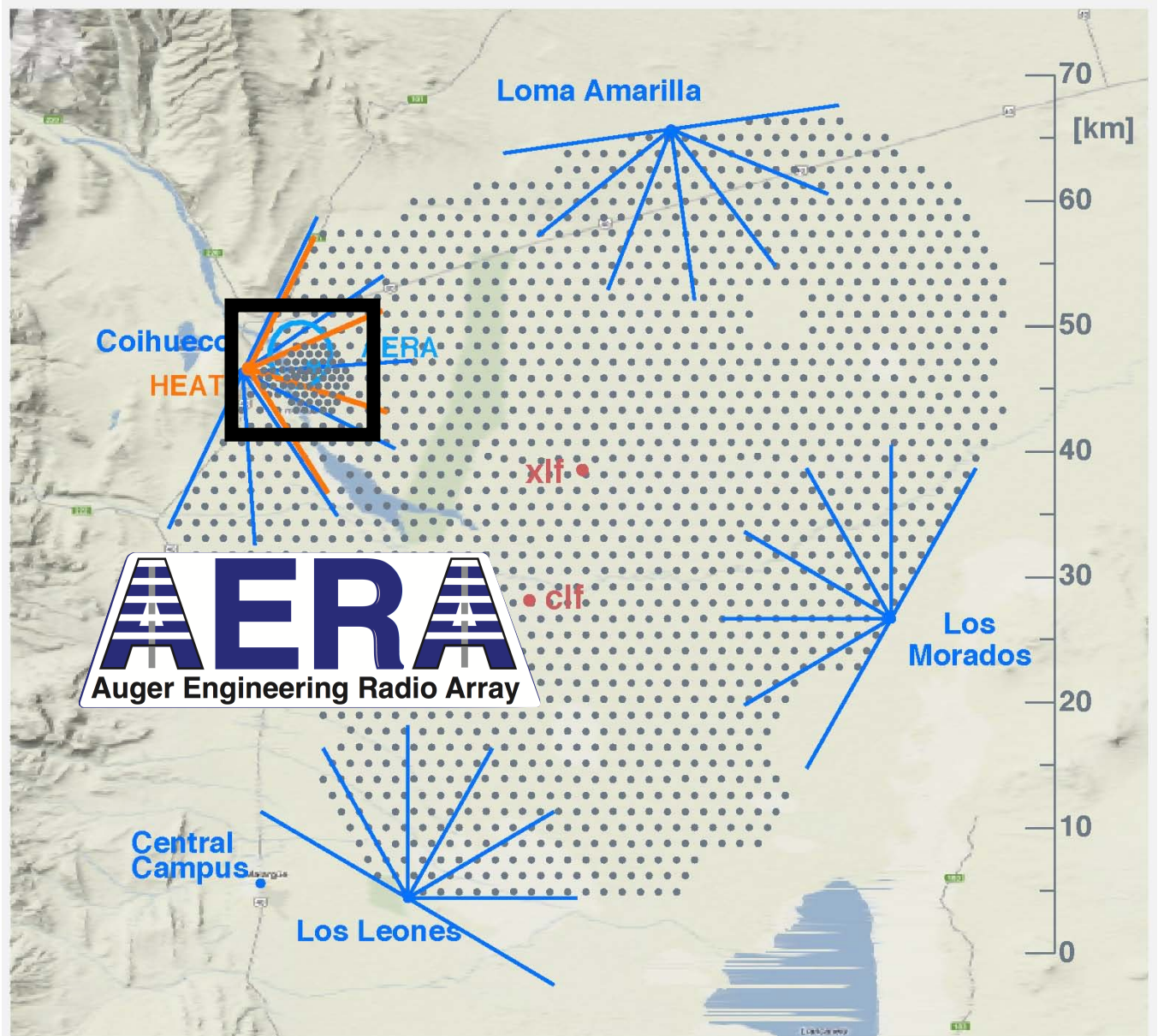
- Located in Malargüe, Argentina
- world's largest cosmic ray detector (3000 km^2)
- detection of air showers induced by cosmic rays
 $E > 10^{17} \text{ eV}$
- physics goals
 - sources
 - acceleration mechanisms
 - origin of the cut-off
 - mass composition
- 1660 Cerenkov tanks
- 4 fluorescence sites (27 telescopes)



The Pierre Auger Observatory

- Located in Malargüe, Argentina
- world's largest cosmic ray detector (3000 km^2)
- detection of air showers induced by cosmic rays
 $E > 10^{17} \text{ eV}$
- physics goals
 - sources
 - acceleration mechanisms
 - origin of the cut-off
 - mass composition
- 1660 Cerenkov tanks
- 4 fluorescence sites (27 telescopes)
- 153 radio stations

coincident measurements

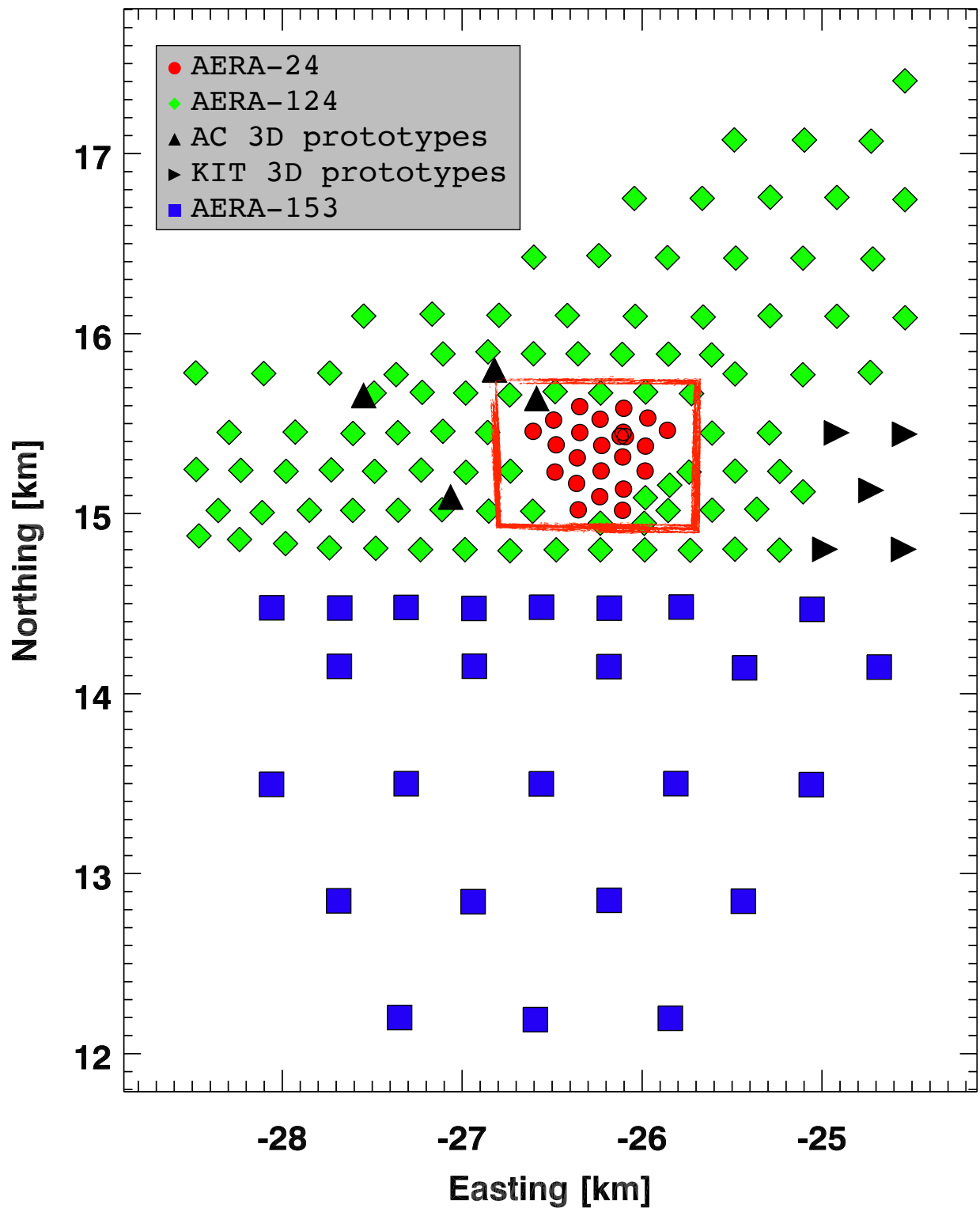


AERA

- Deployment and spacing:
 - 2011: Phase I - 24 stations - 144 m



log-periodic antenna

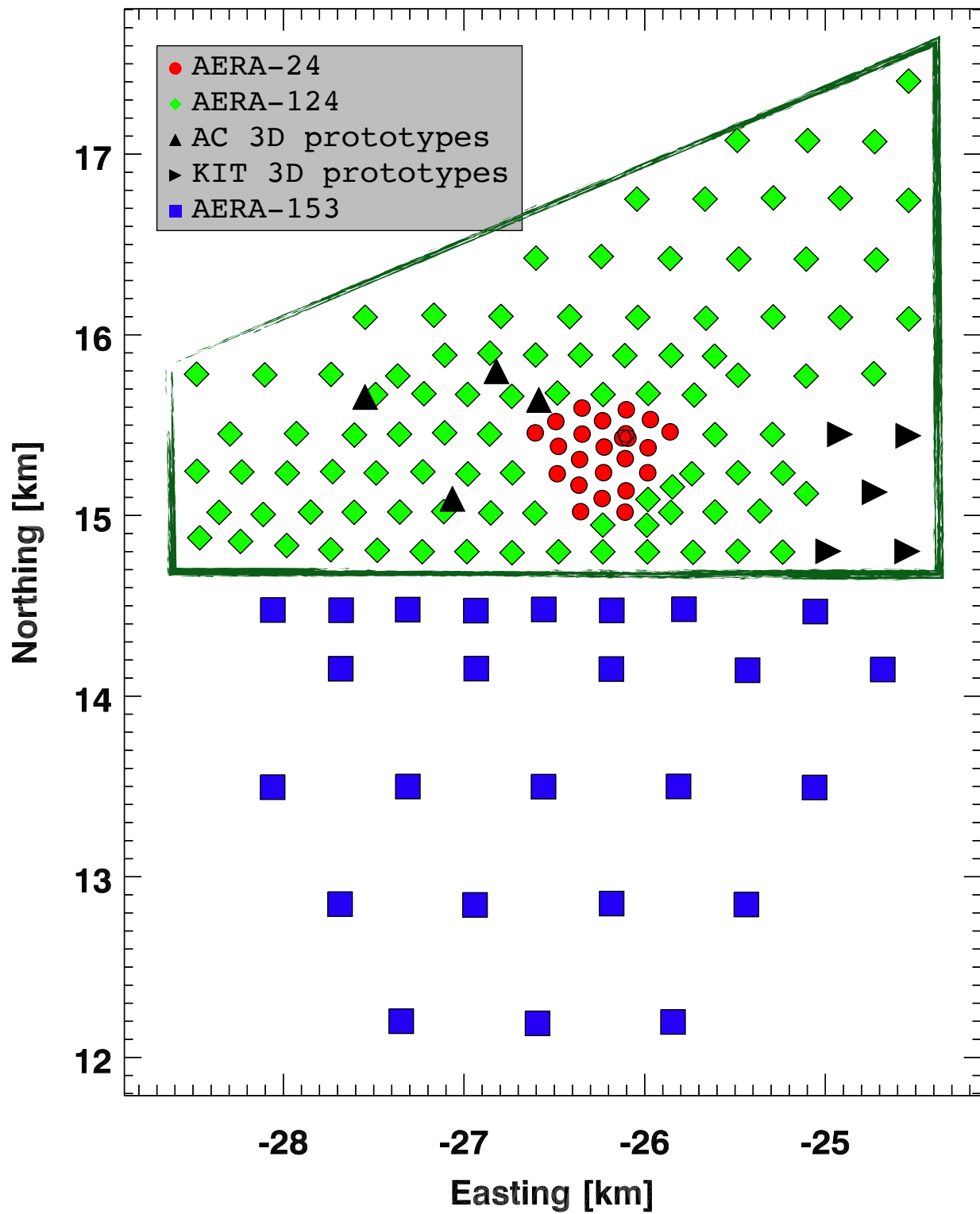


AERA

- Deployment and spacing:
 - 2011: Phase I - 24 stations - 144 m
 - 2013: Phase II - 124 stations - 250 & 375 m



butterfly antenna

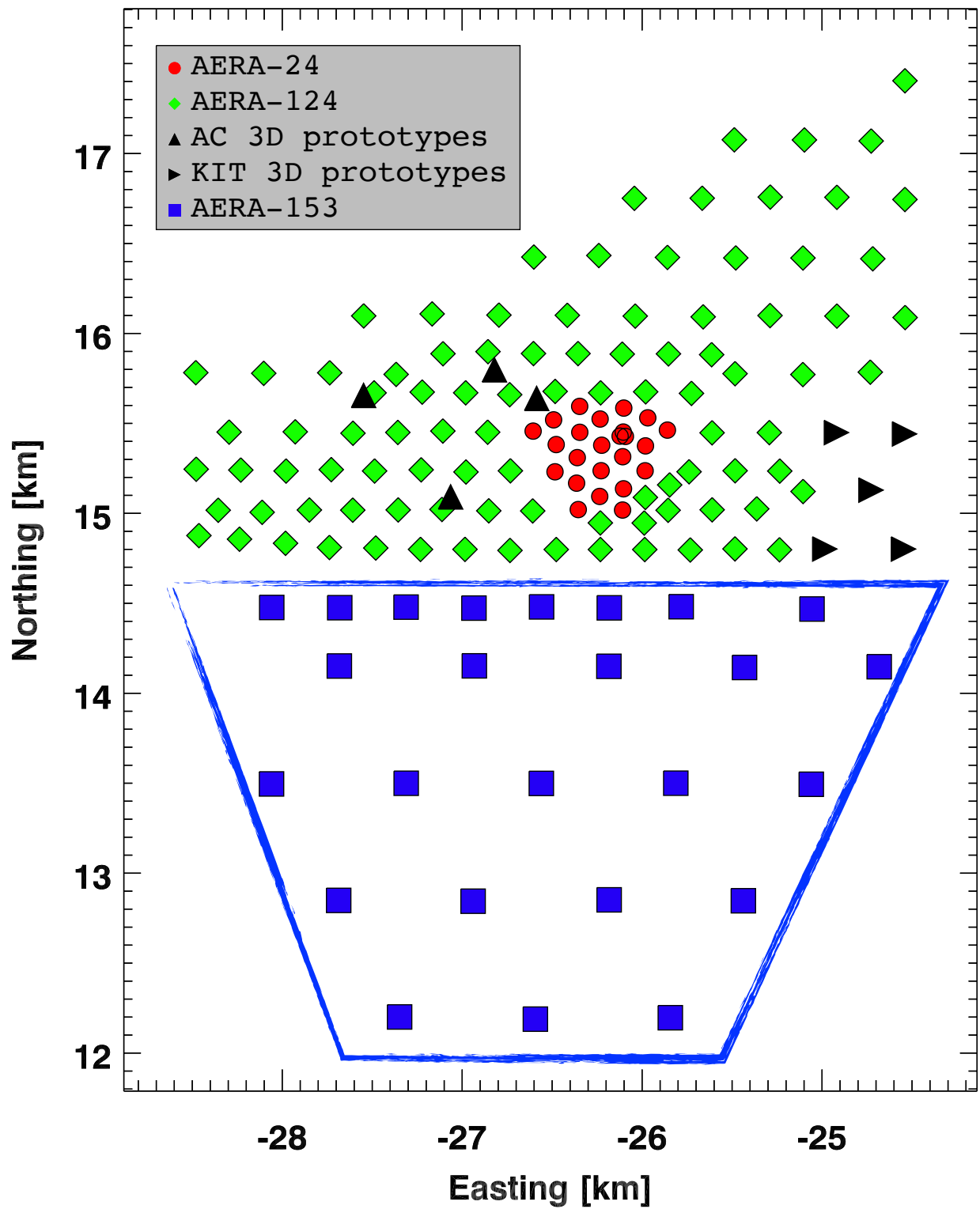


AERA

- Deployment and spacing:
 - 2011: Phase I - 24 stations - 144 m
 - 2013: Phase II - 124 stations - 250 & 375 m
 - 2015: Phase III - 153 stations - 750 m

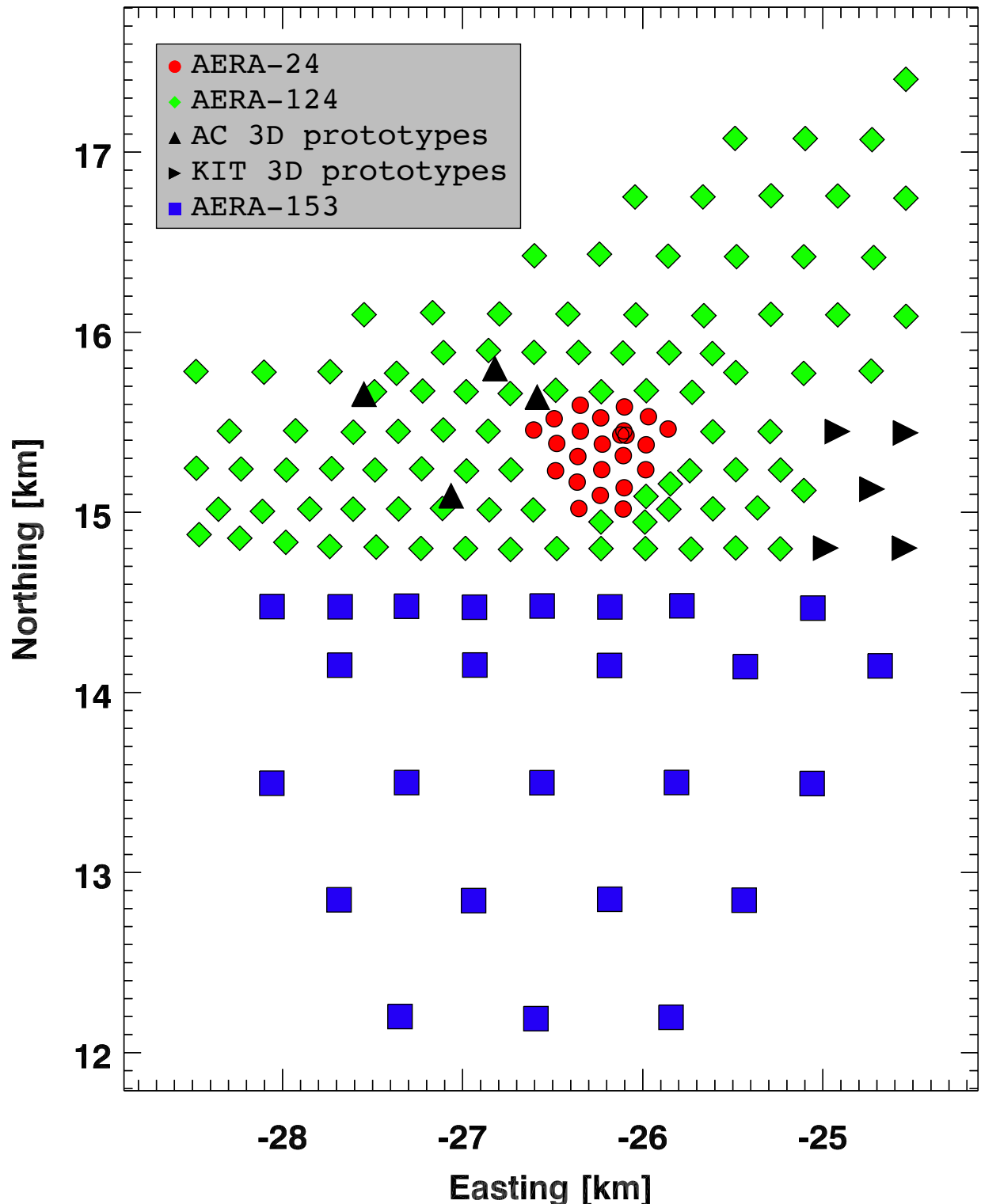


butterfly antenna



AERA

- Deployment and spacing:
 - 2011: Phase I - 24 stations - 144 m
 - 2013: Phase II - 124 stations - 250 & 375 m
 - 2015: Phase III - 153 stations - 750 m
- 153 radio stations on 17 km²
- calibrated in time and amplitude
- duty cycle ~100%
- 30 - 80 MHz
- two horizontal polarizations
- energy range: $E > 10^{17}$ eV
- shower physics:
 - arrival direction
 - core position
 - energy
 - mass composition



Emission mechanisms

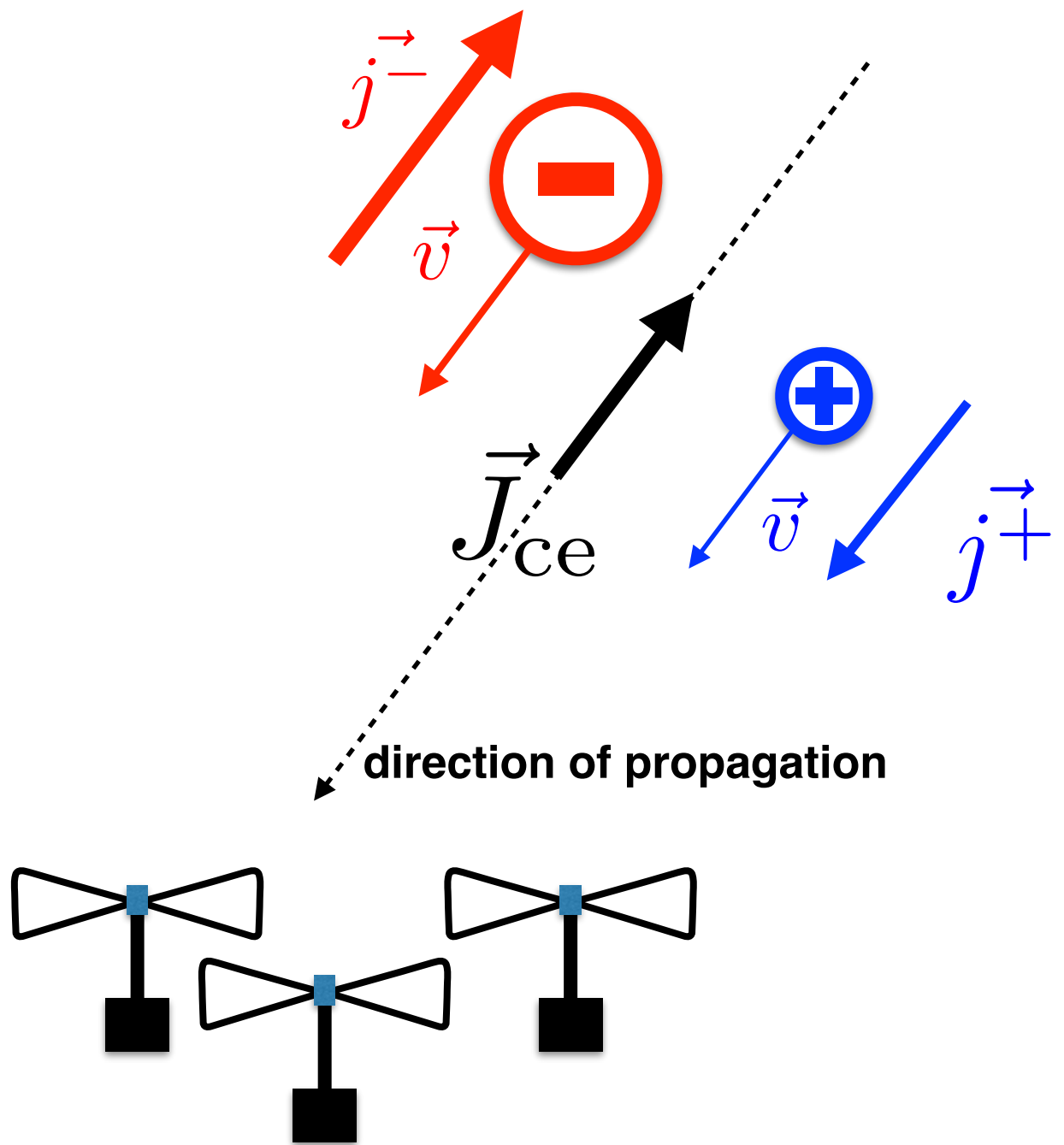
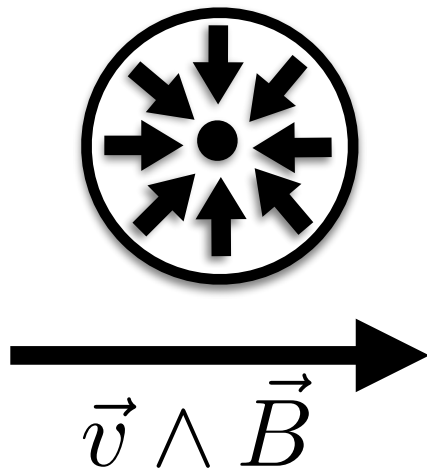
- Charge excess mechanism

Excess of negative charges

$$\vec{J}_{ce} = \vec{j}^- + \vec{j}^+$$

$$\vec{E}_{ce}(t) \propto \frac{\partial}{\partial t} \vec{J}_{ce}(t)$$

Radially polarized around shower axis



Emission mechanisms

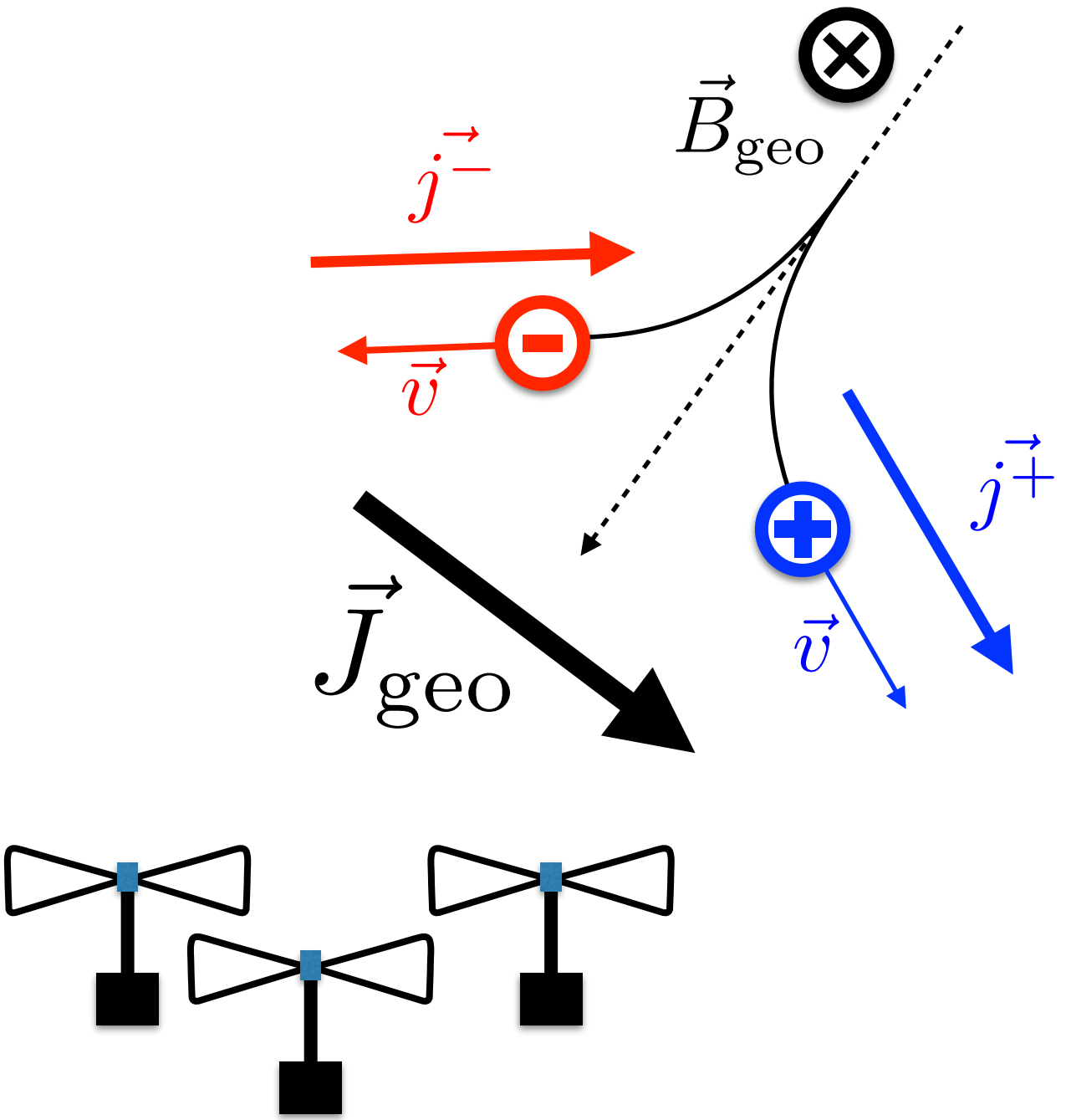
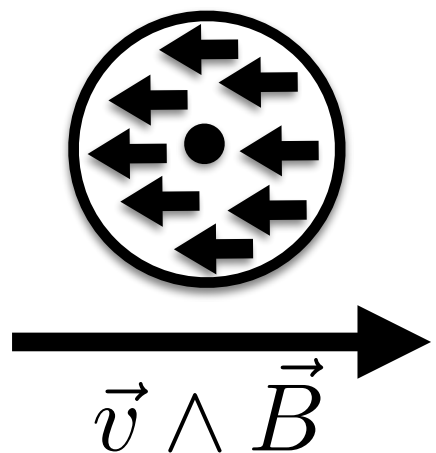
- Geomagnetic mechanism

Lorentz force applied to secondary particles

$$\vec{J}_{\text{geo}} = \vec{j}^- + \vec{j}^+$$

$$\vec{E}_{\text{geo}}(t) \propto \frac{\partial}{\partial t} \vec{J}_{\text{geo}}(t)$$

Polarized in the direction of the Lorentz force

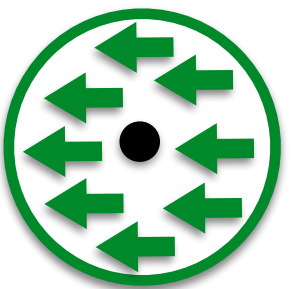


Emission mechanisms

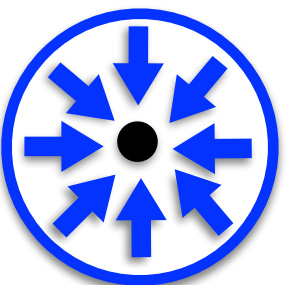
- Total electric field

composition of the two effects

geomagnetic



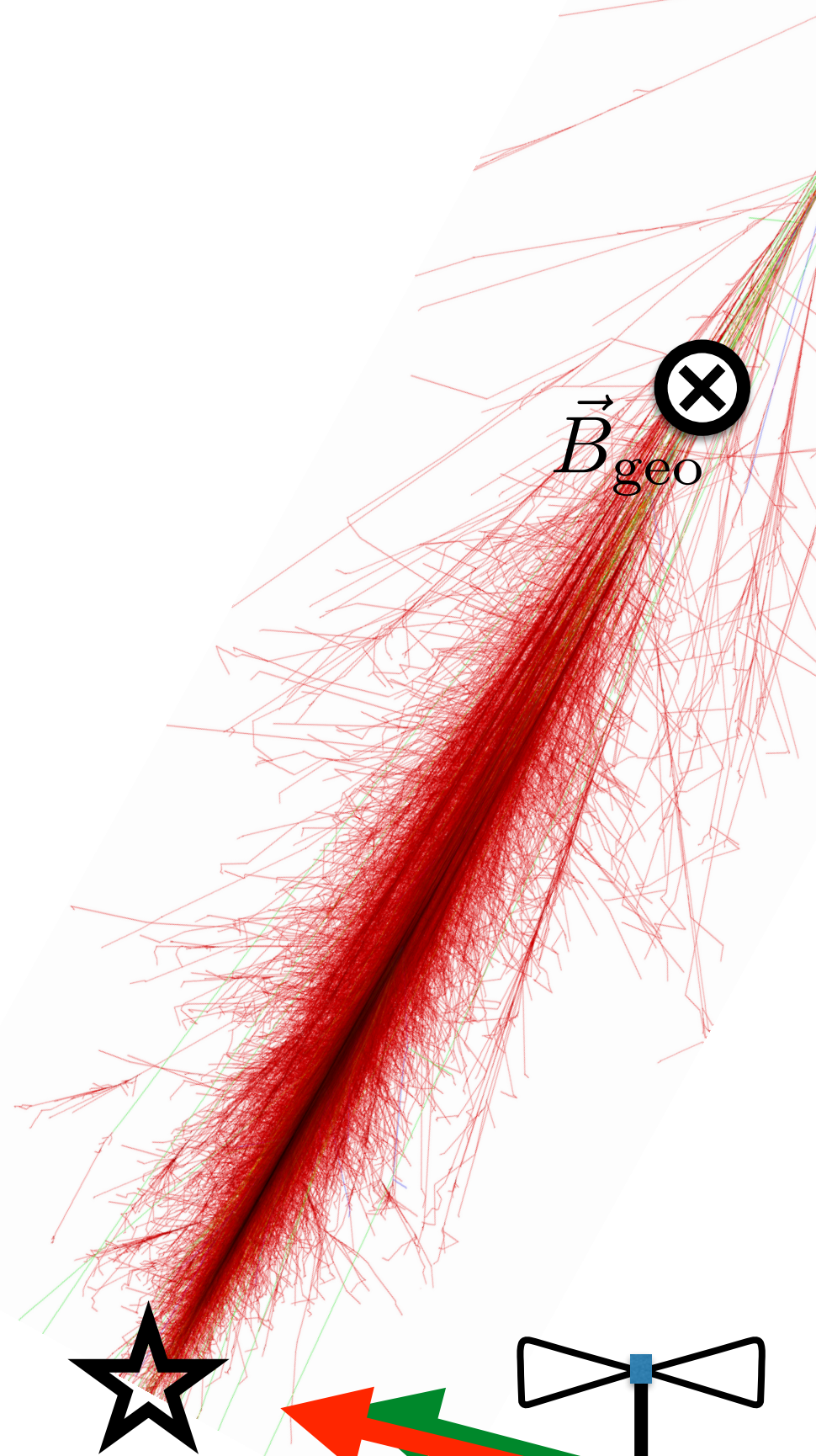
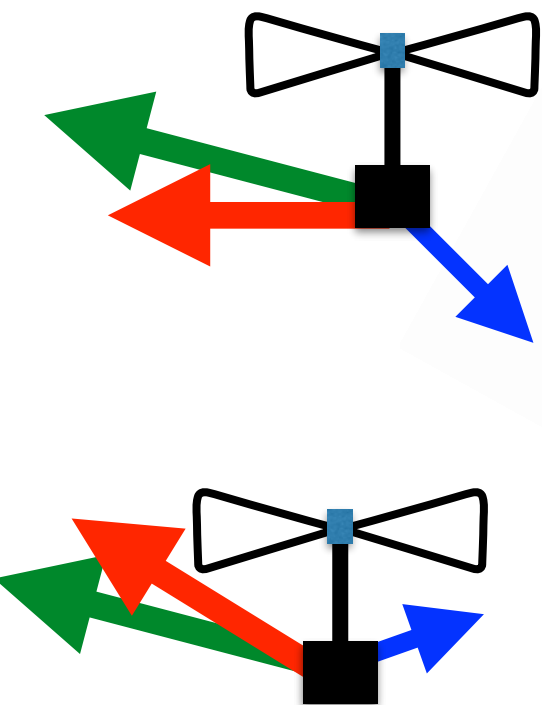
charge excess



$$+$$

 $\vec{v} \wedge \vec{B}$

leads to asymmetry around the shower axis and complex pattern at the ground level:

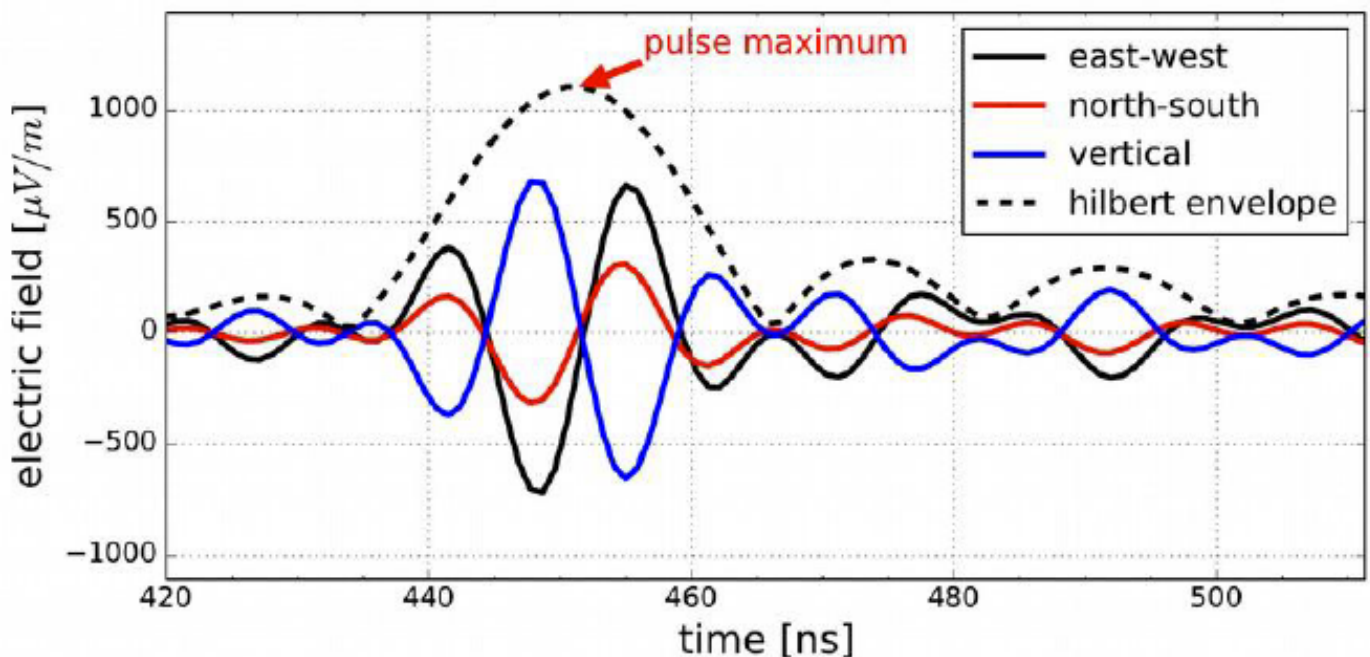


Energy measurement

compute the total electric field from the three polarization components

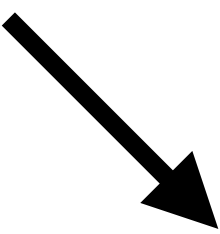
with vertical polarization from the arrival direction

electric field Vs time

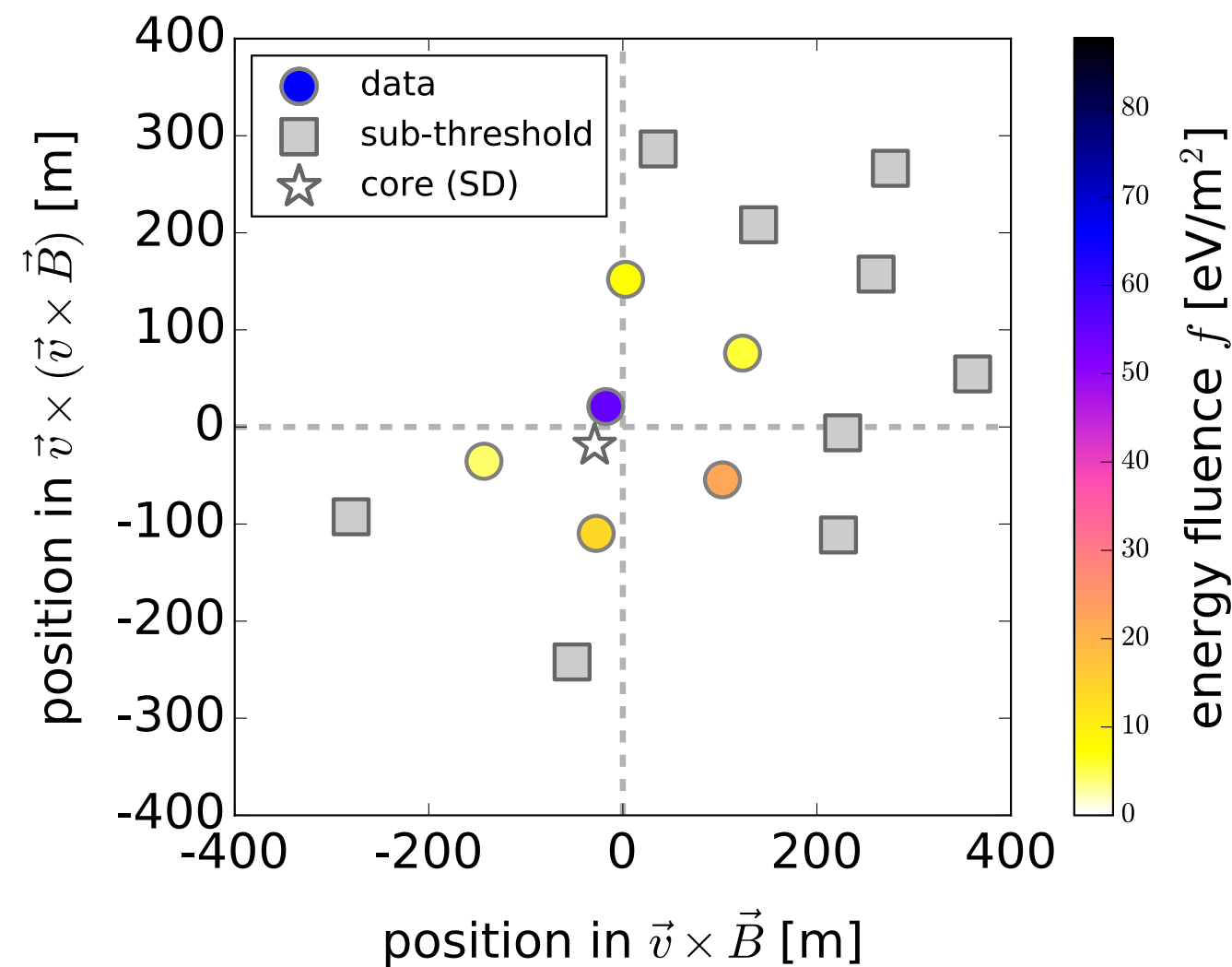


energy estimator calculated for all stations

Integration of the Poynting vector over time



energy
fluence
(eV/m^2)

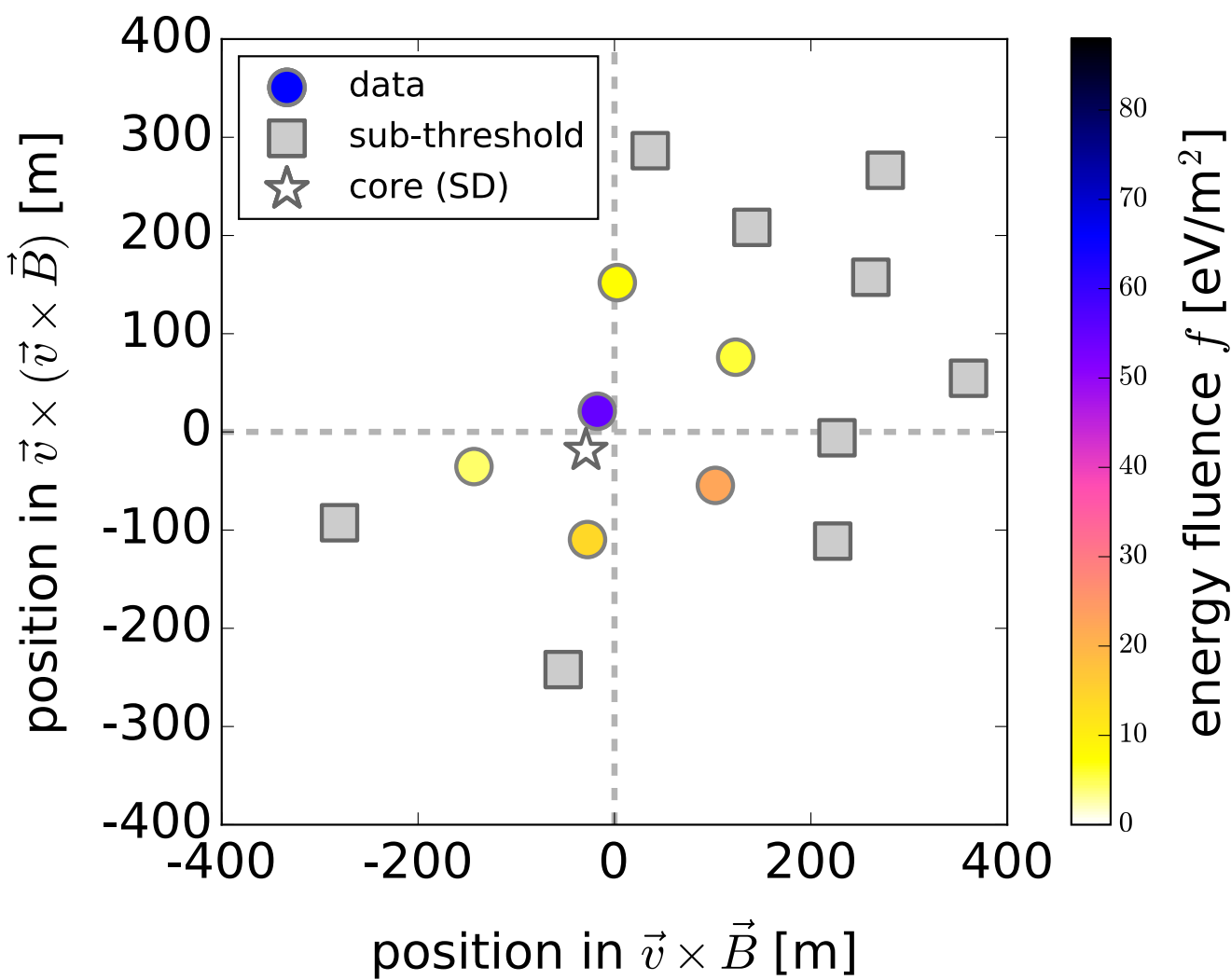


Energy measurement

Fit a 2D model that accounts for asymmetry around the shower axis

$$\text{LDF}(\mathbf{r}) = A \left[\exp \left(\frac{-(\mathbf{r} + C_1 \mathbf{e}_{\mathbf{v} \times \mathbf{B}} - \mathbf{r}_{\text{core}})^2}{\sigma} \right) - C_0 \exp \left(\frac{-(\mathbf{r} + C_2 \mathbf{e}_{\mathbf{v} \times \mathbf{B}} - \mathbf{r}_{\text{core}})}{(C_3 e^{C_4 \sigma})^2} \right) \right]$$

Nelles et al., Astropart. Phys. 60, 13 (2015)

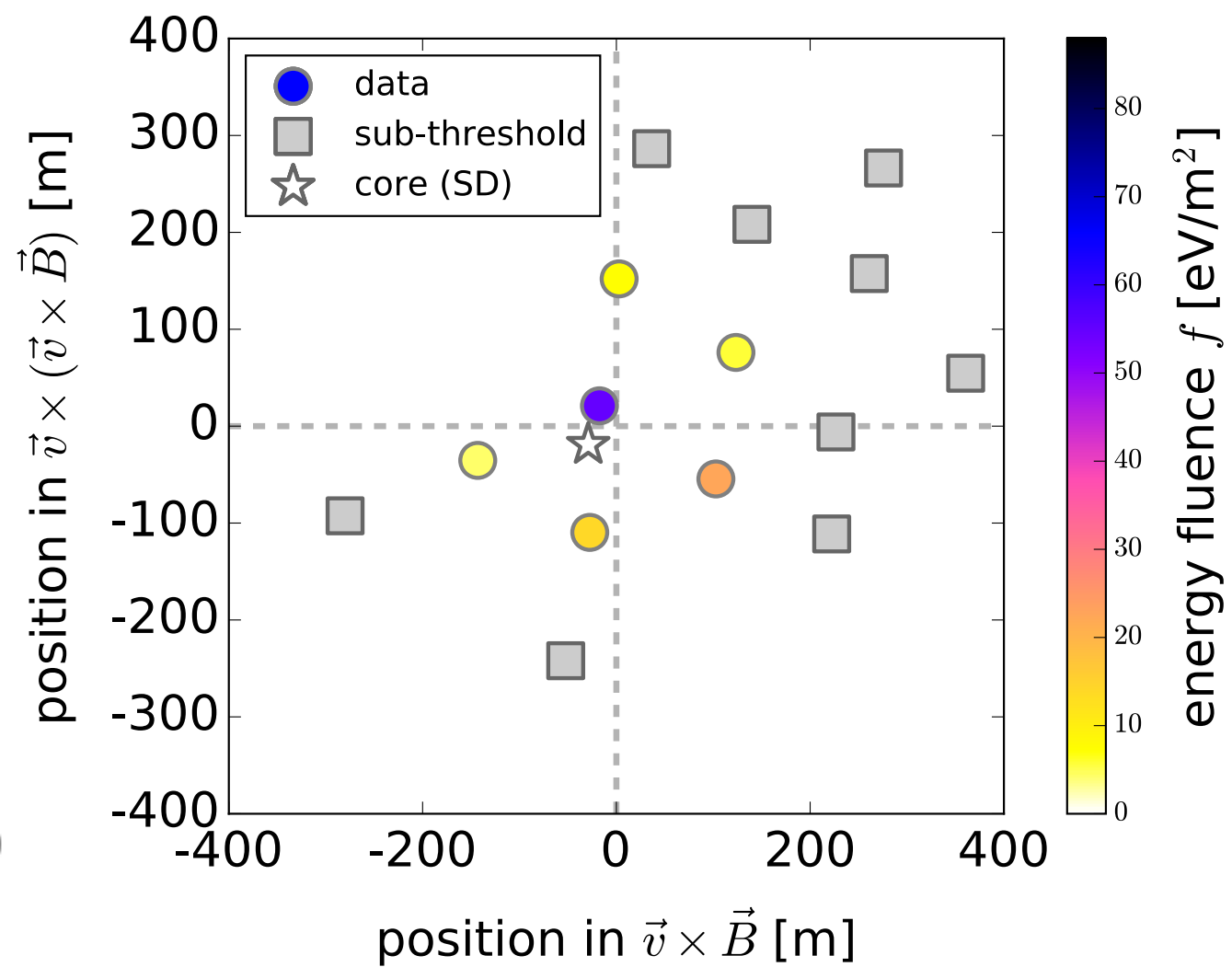
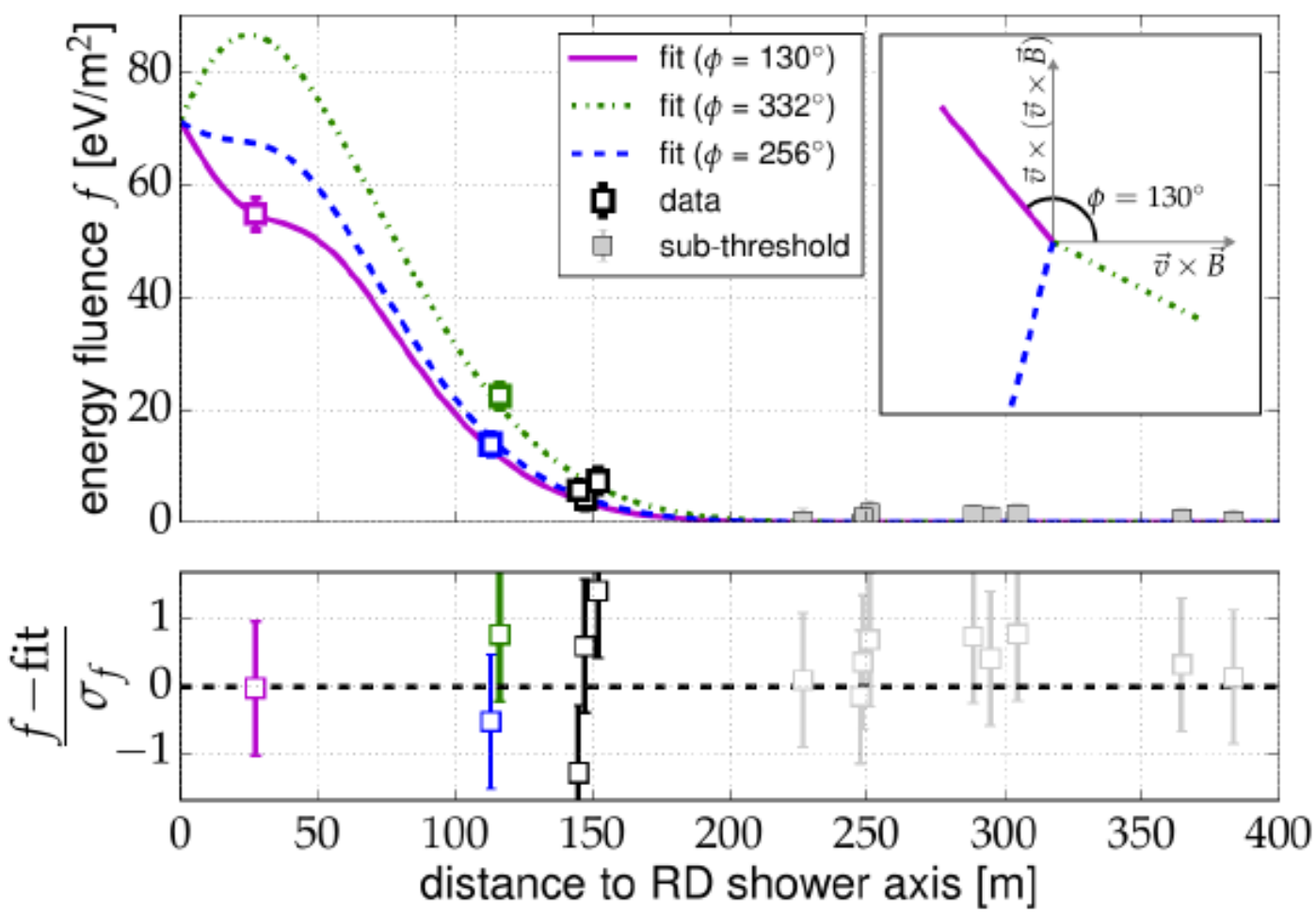


Energy measurement

Fit a 2D model that accounts for asymmetry around the shower axis

$$\text{LDF}(\mathbf{r}) = A \left[\exp \left(\frac{-(\mathbf{r} + C_1 \mathbf{e}_{\mathbf{v} \times \mathbf{B}} - \mathbf{r}_{\text{core}})^2}{\sigma} \right) - C_0 \exp \left(\frac{-(\mathbf{r} + C_2 \mathbf{e}_{\mathbf{v} \times \mathbf{B}} - \mathbf{r}_{\text{core}})}{(C_3 e^{C_4 \sigma})^2} \right) \right]$$

Nelles et al., Astropart. Phys. 60, 13 (2015)



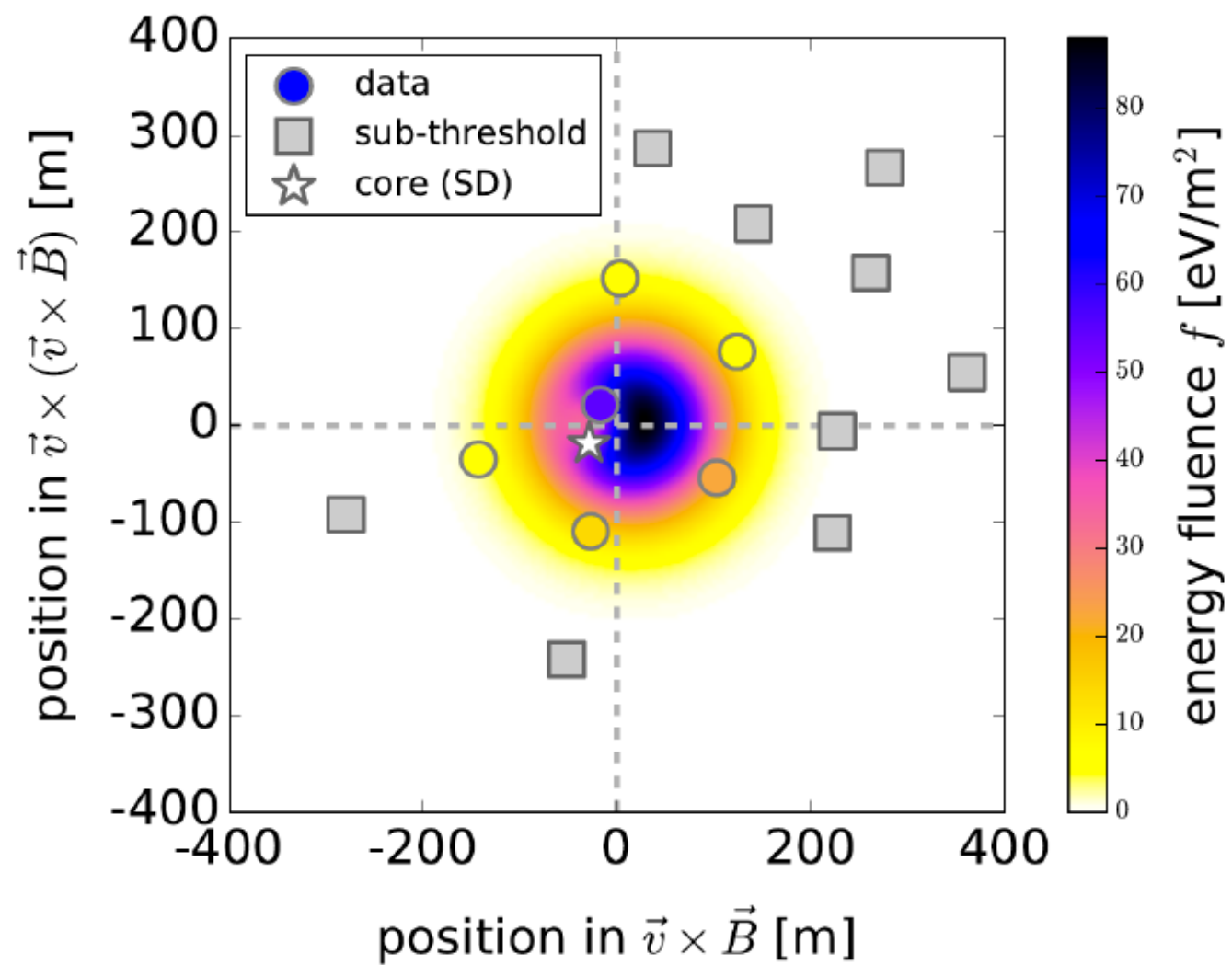
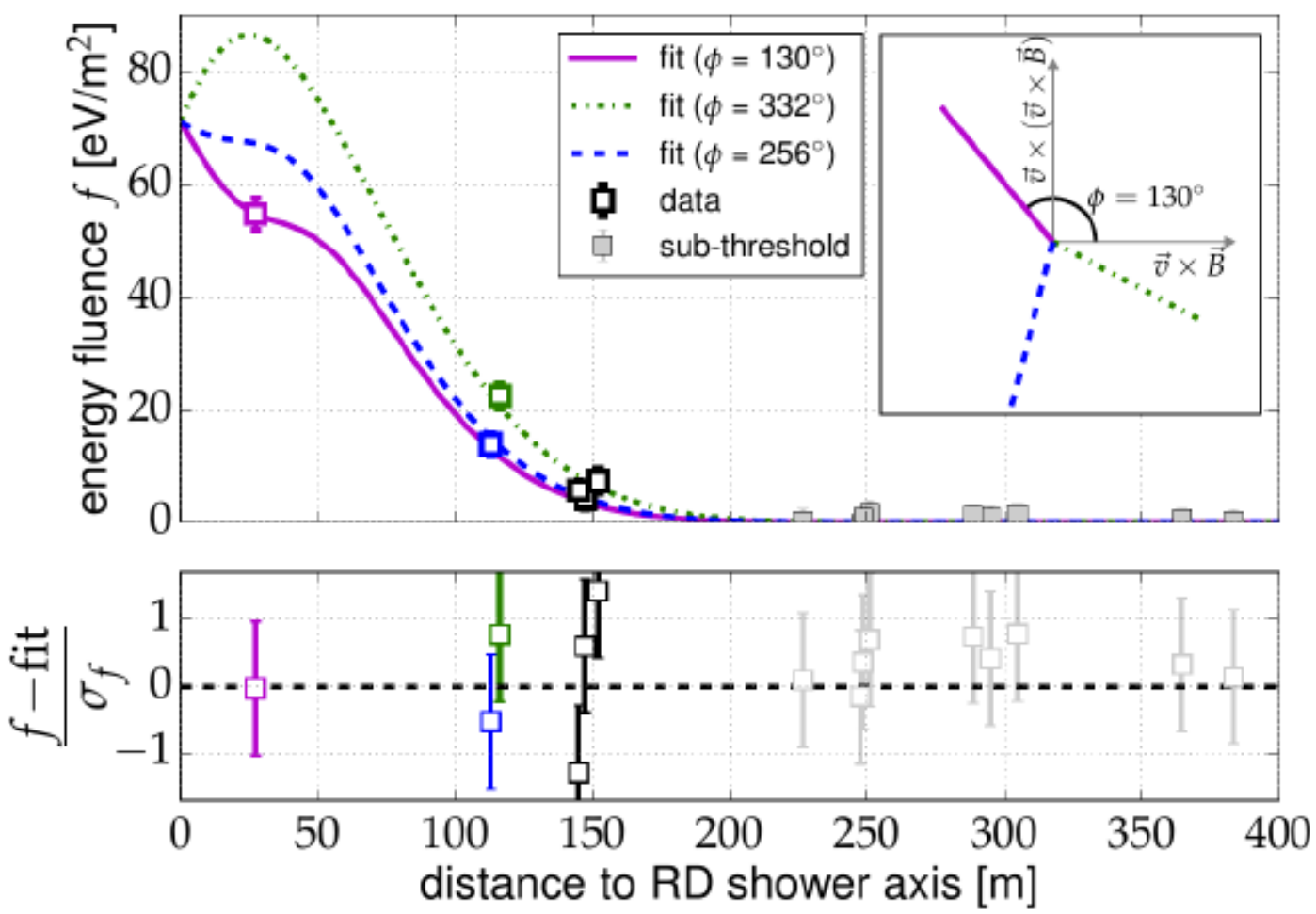
Energy measurement

Fit a 2D model that accounts for asymmetry around the shower axis

$$\text{LDF}(\mathbf{r}) = A \left[\exp \left(\frac{-(\mathbf{r} + C_1 \mathbf{e}_{\mathbf{v} \times \mathbf{B}} - \mathbf{r}_{\text{core}})^2}{\sigma} \right) - C_0 \exp \left(\frac{-(\mathbf{r} + C_2 \mathbf{e}_{\mathbf{v} \times \mathbf{B}} - \mathbf{r}_{\text{core}})}{(C_3 e^{C_4 \sigma})^2} \right) \right]$$

Nelles et al., Astropart. Phys. 60, 13 (2015)

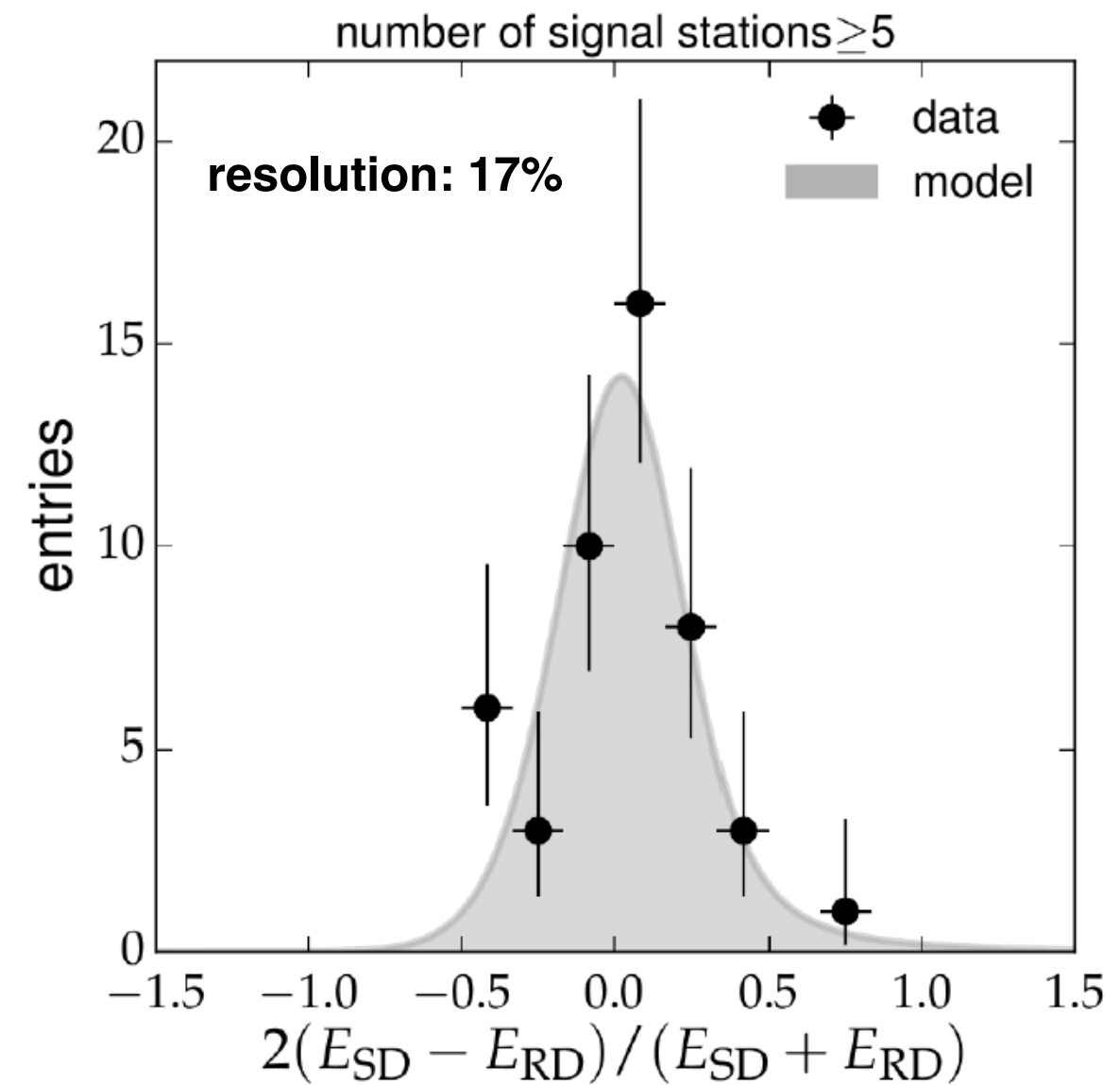
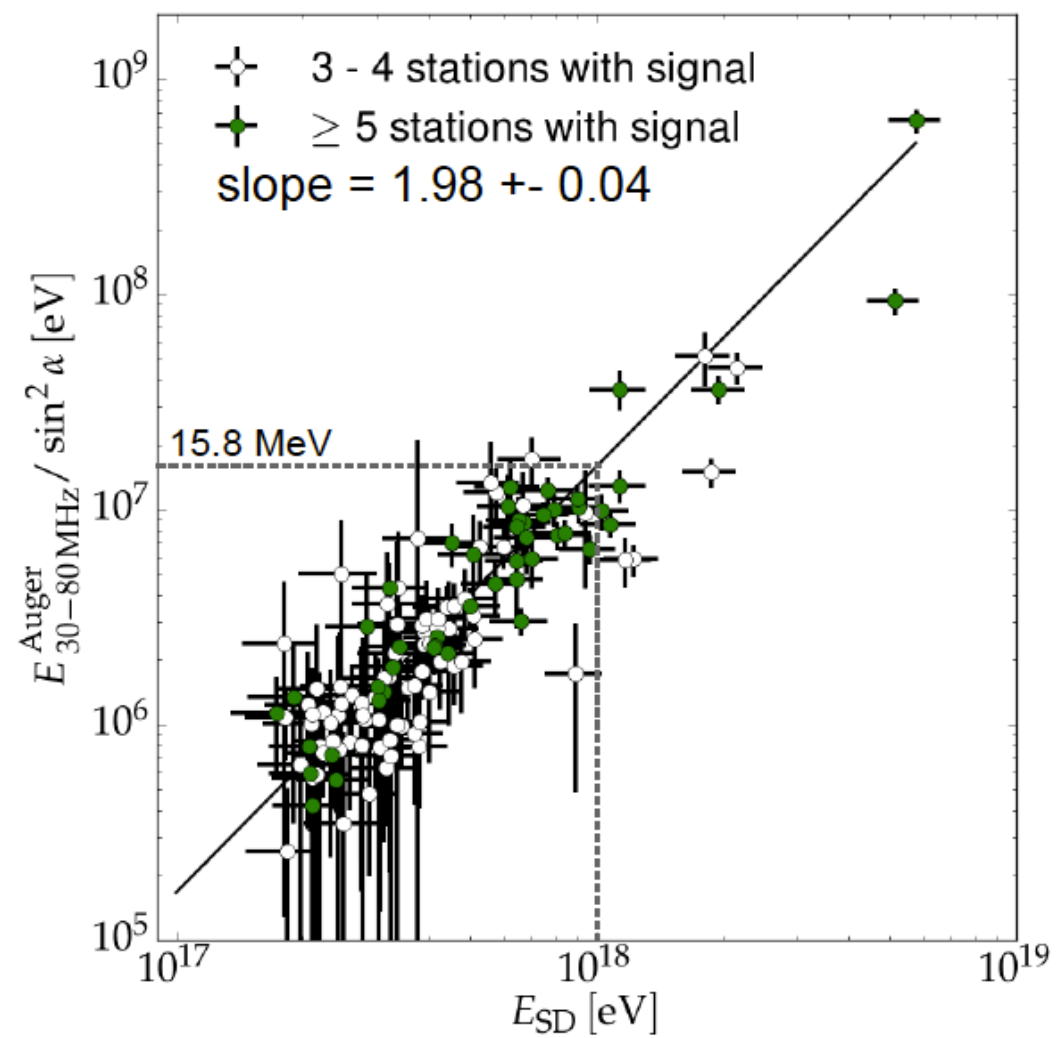
$$E_{\text{radio}} = \iint \text{LDF}(x, y) \, dx \, dy$$



Energy measurement

Correlation between the deposited radio energy and SD energy for coincident measurements

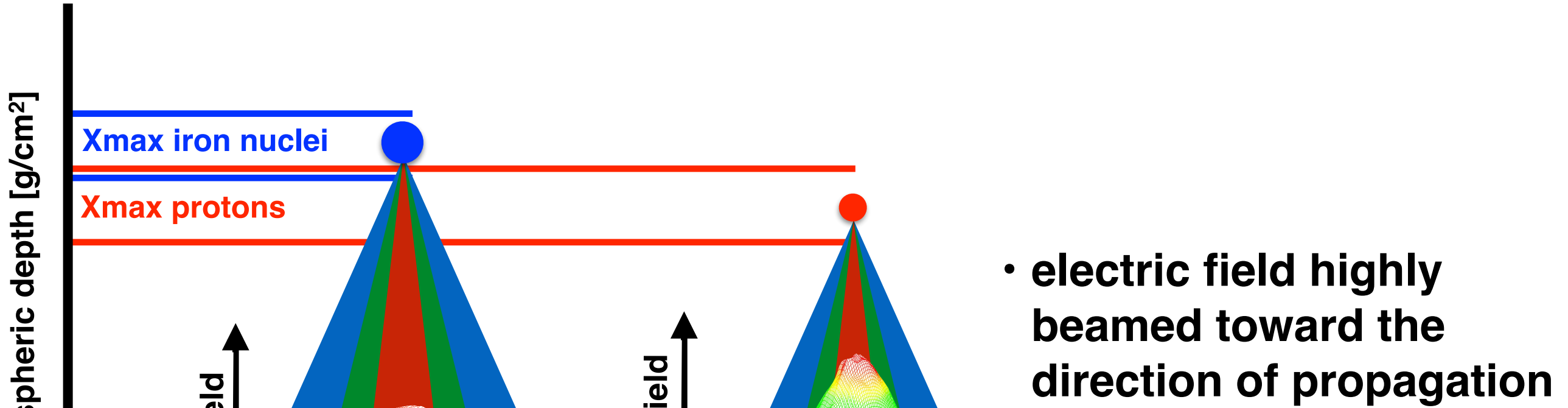
Auger collab., PRL 116, 241101 (2016)
Auger collab., PRD 93, 122005 (2016)



Energy measurement from radio signal!

Mass composition

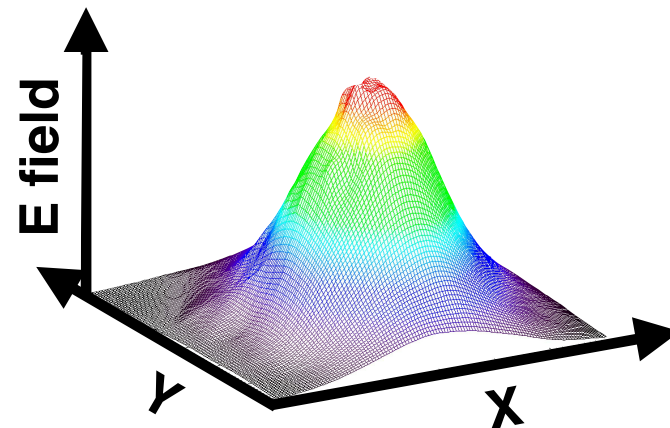
- Xmax correlated to the mass of the primary



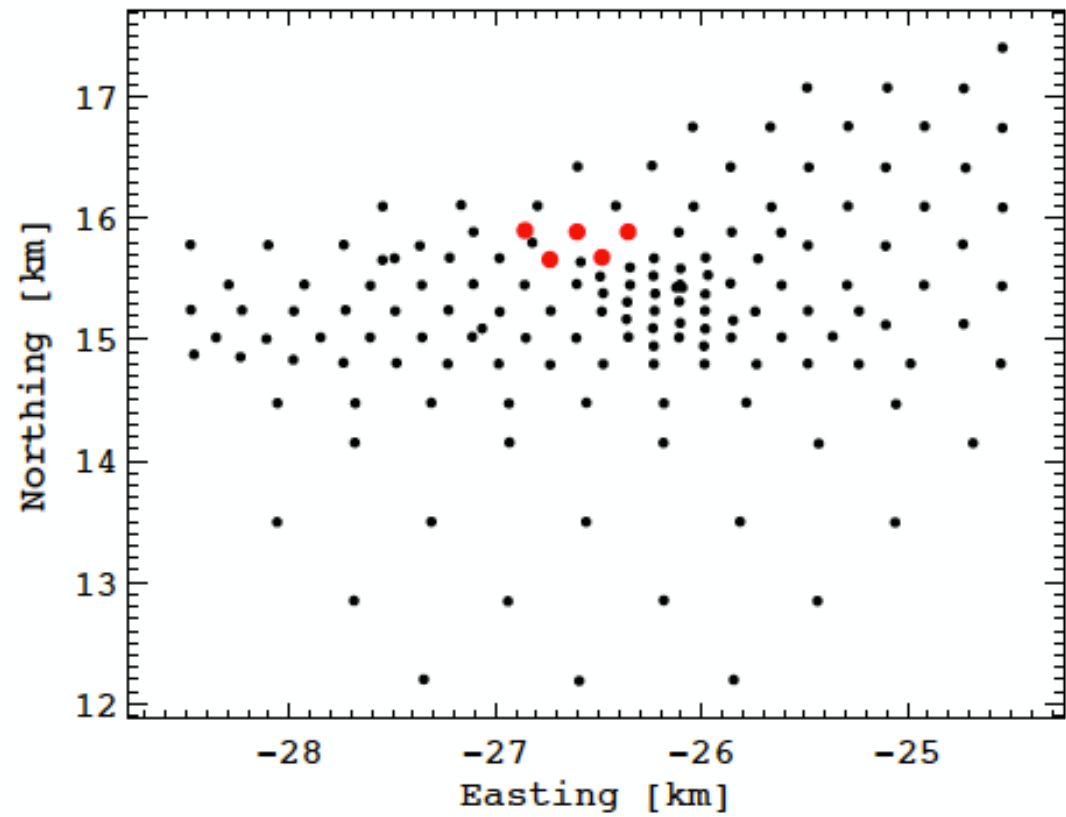
- strong correlation between the LDF and Xmax
- Xmax reconstruction from the amplitude or energy fluence with a duty cycle close to 100% (14% for fluorescence)

Mass composition

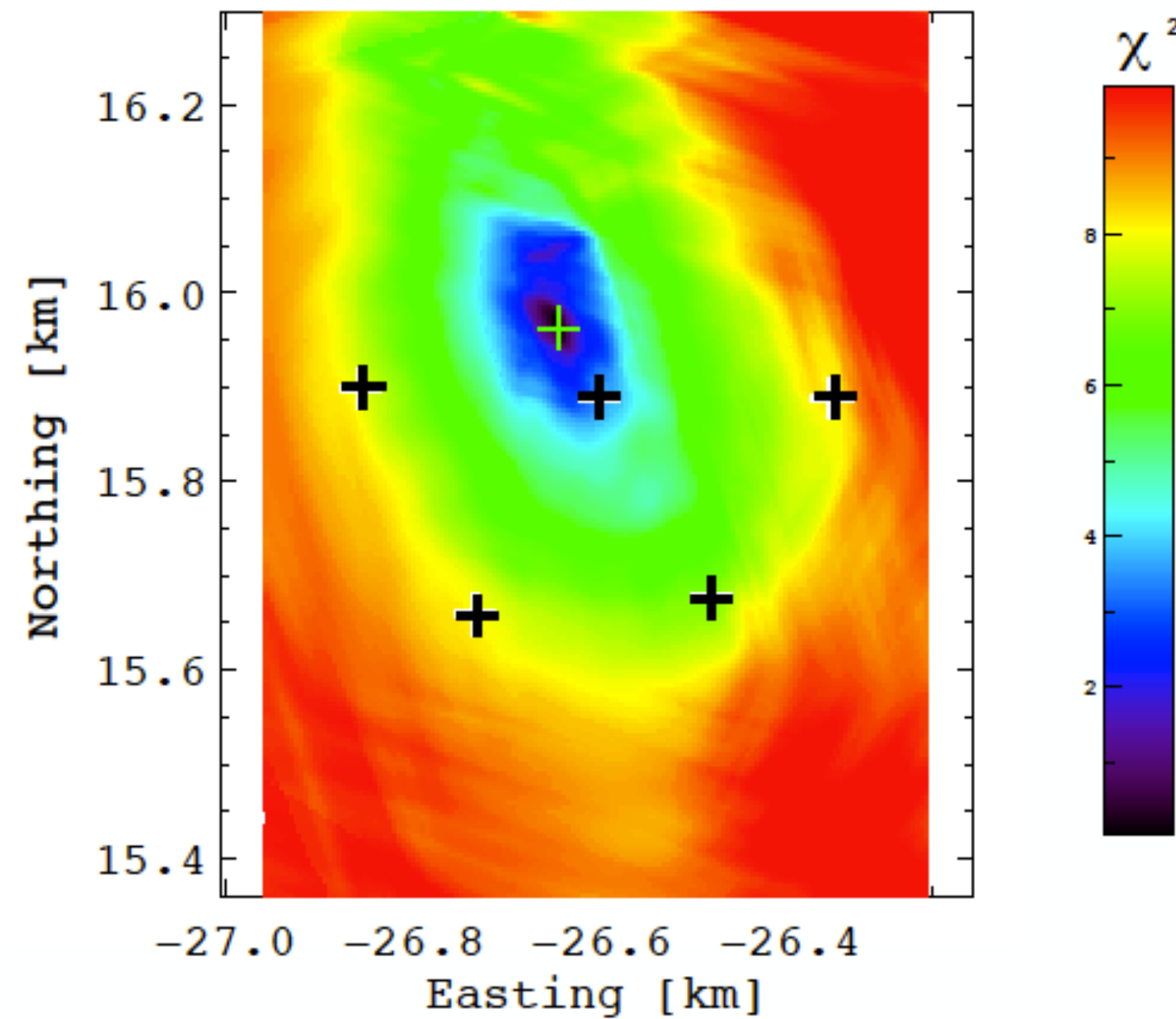
- Simulation of few LDF (radio arrival direction)



- compare simulation to data

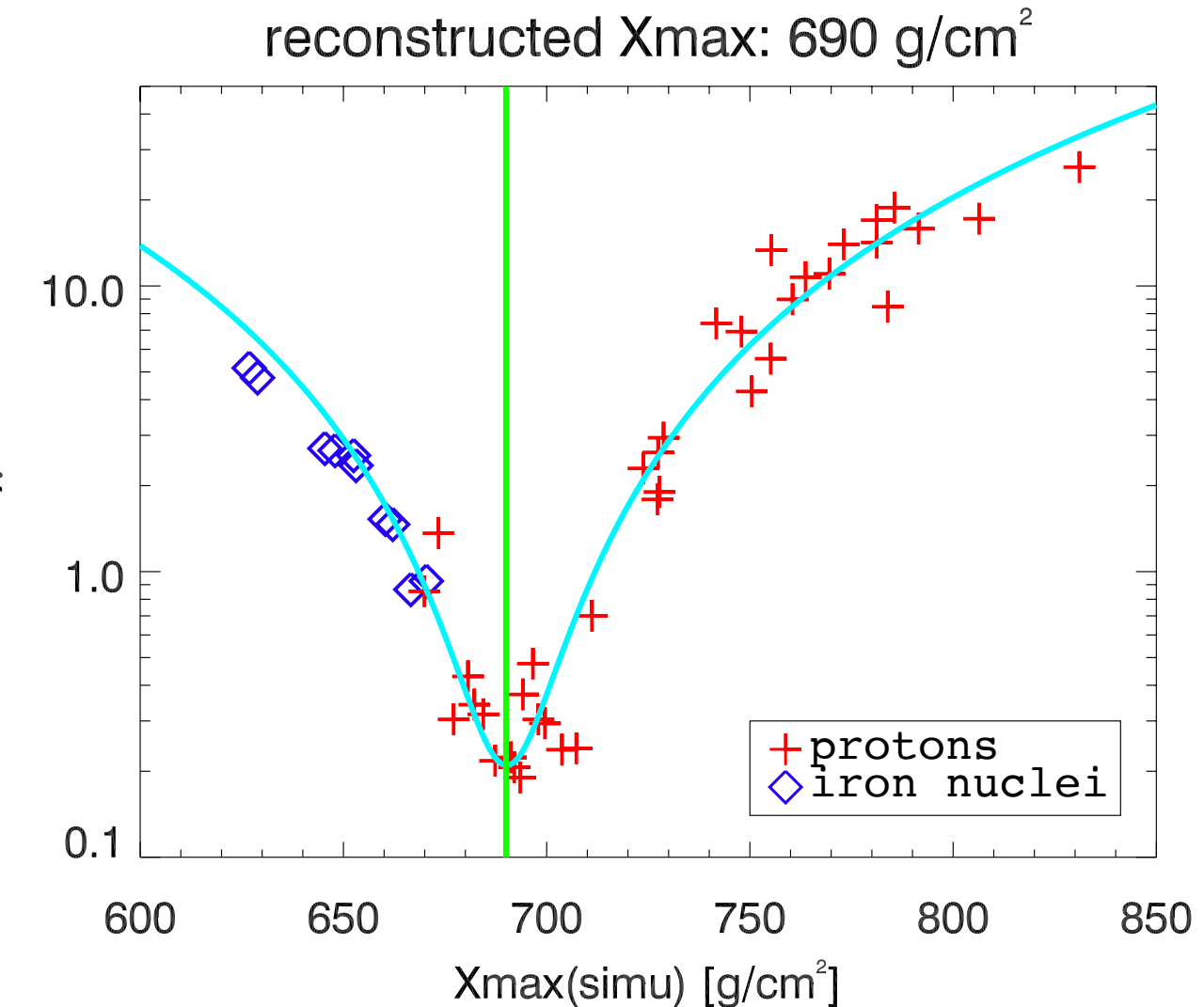
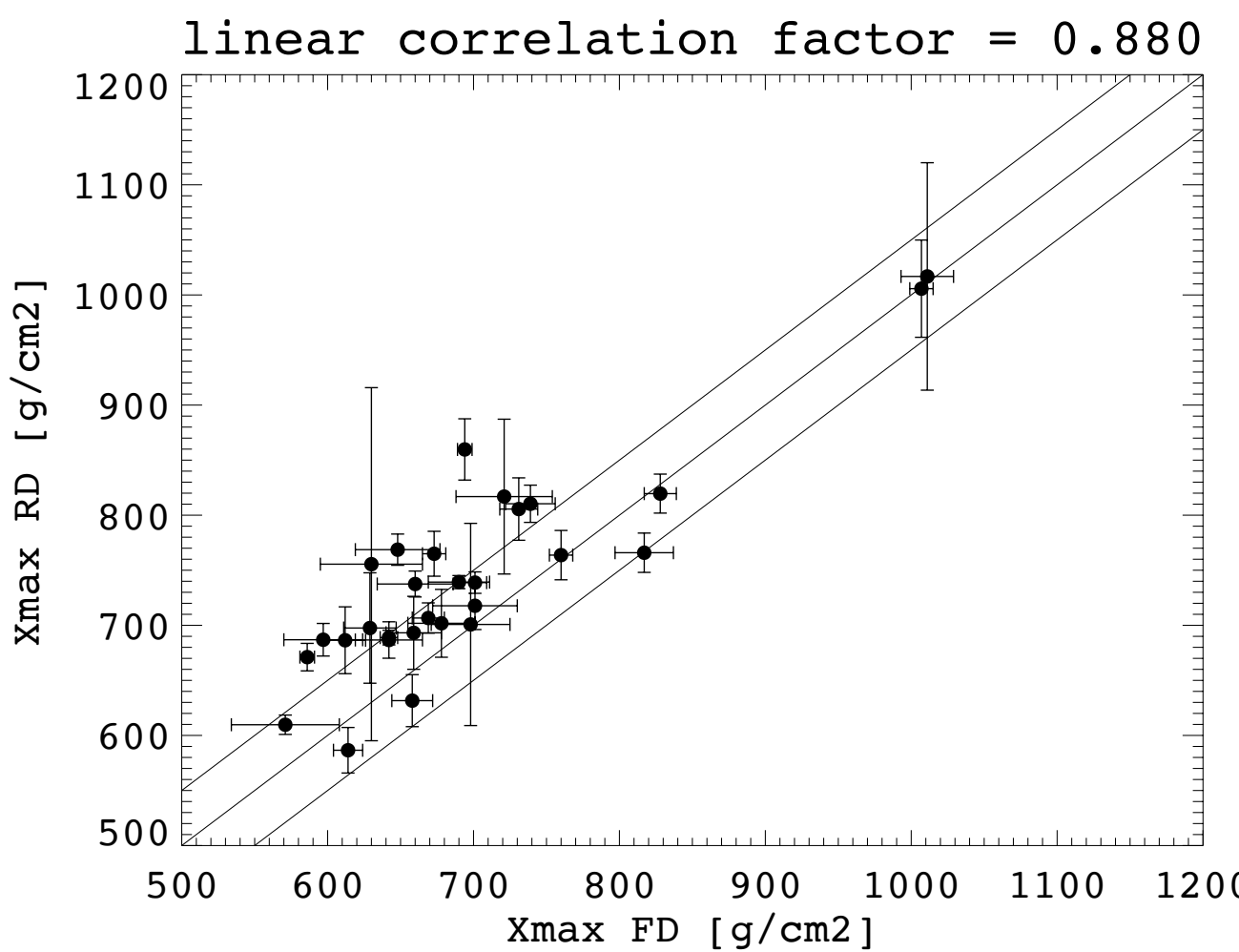


- the agreement is tested for different locations of the simulated core position to find best core position



Mass composition

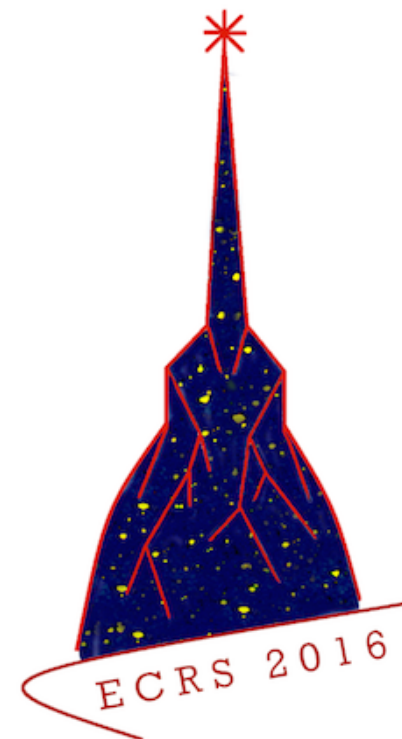
- Montecarlo on Xmax values
- Best agreement for an optimal Xmax
- Comparison to FD measurements



- 4 methods developed for AERA
- width of the residuals ~40g/cm²

Conclusions

- AERA produces high-quality data in coincidence with the fluorescence and ground detectors
- The emission mechanisms of the radio signal are now well understood
- Energy:
 - the primary energy is partly released as radiation energy in a calorimetric way
 - the energy resolution using the radio signal is 17%
 - this provides a new independent energy scale for CR experiments
- Composition:
 - we work on systematic Xmax reconstruction with a 100% duty cycle
 - The expected resolution is of 40 g/cm^2
- Current analysis are focused on determining the energy spectrum and mass composition in the transition region

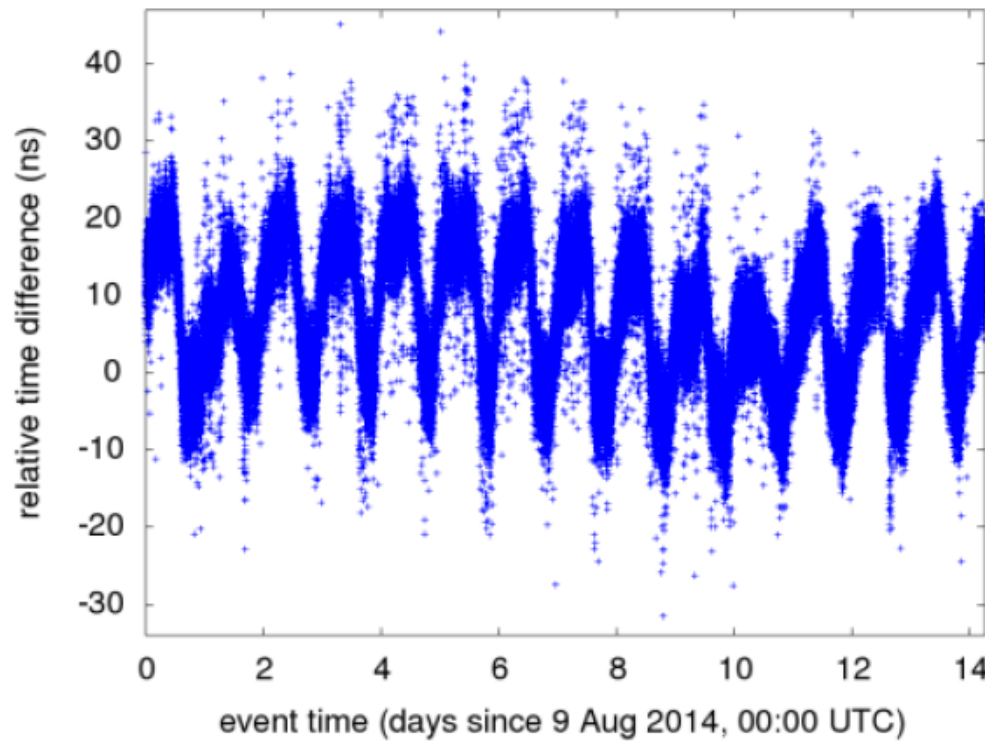


Thank you for your attention!

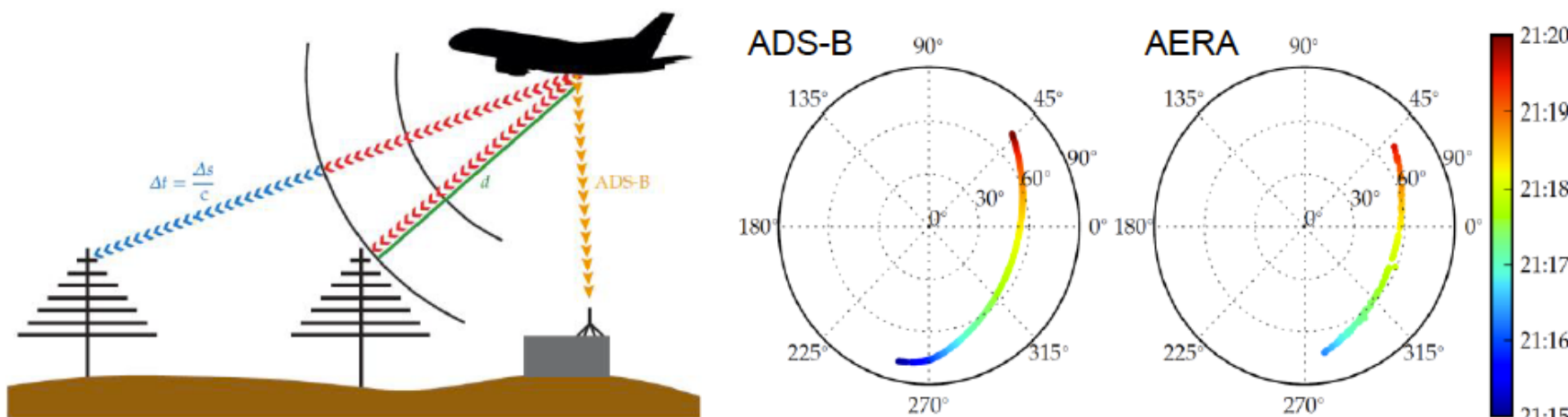
Time calibration

- Beacon method:

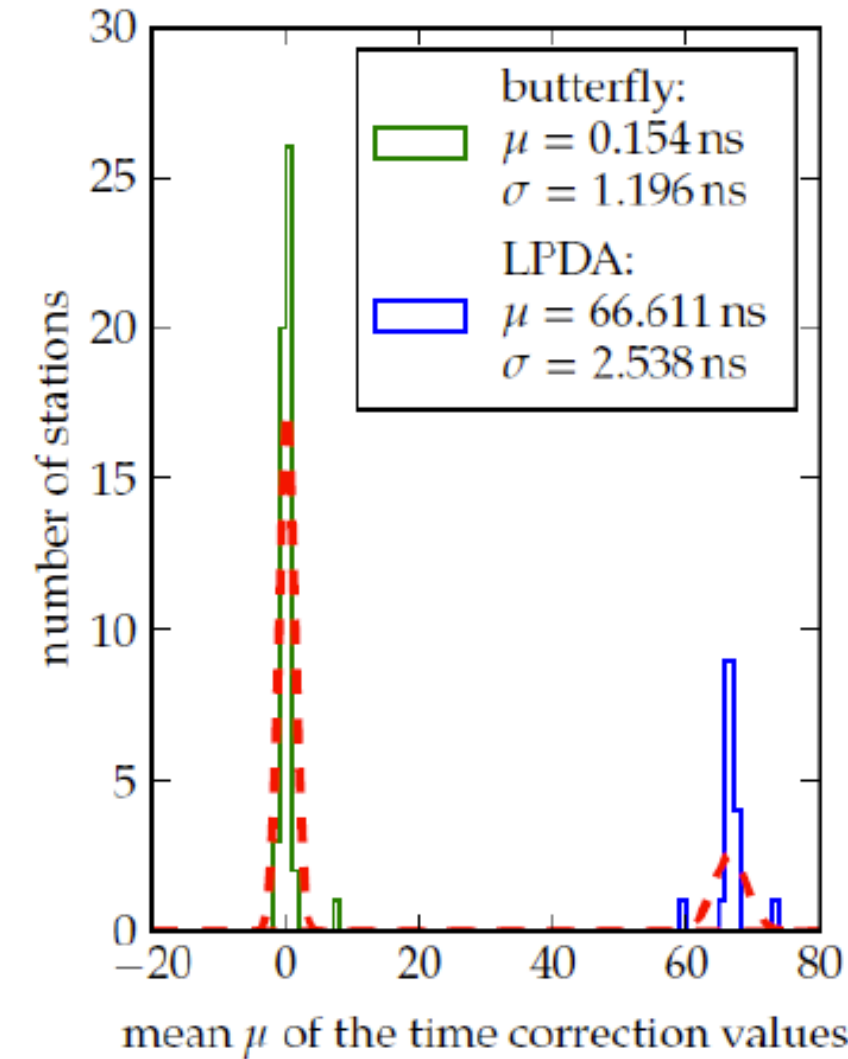
frequencies:
58MHz, 61MHz,
68MHz, 71MHz



- Air plane method: ADS-B + radio signal from air plane



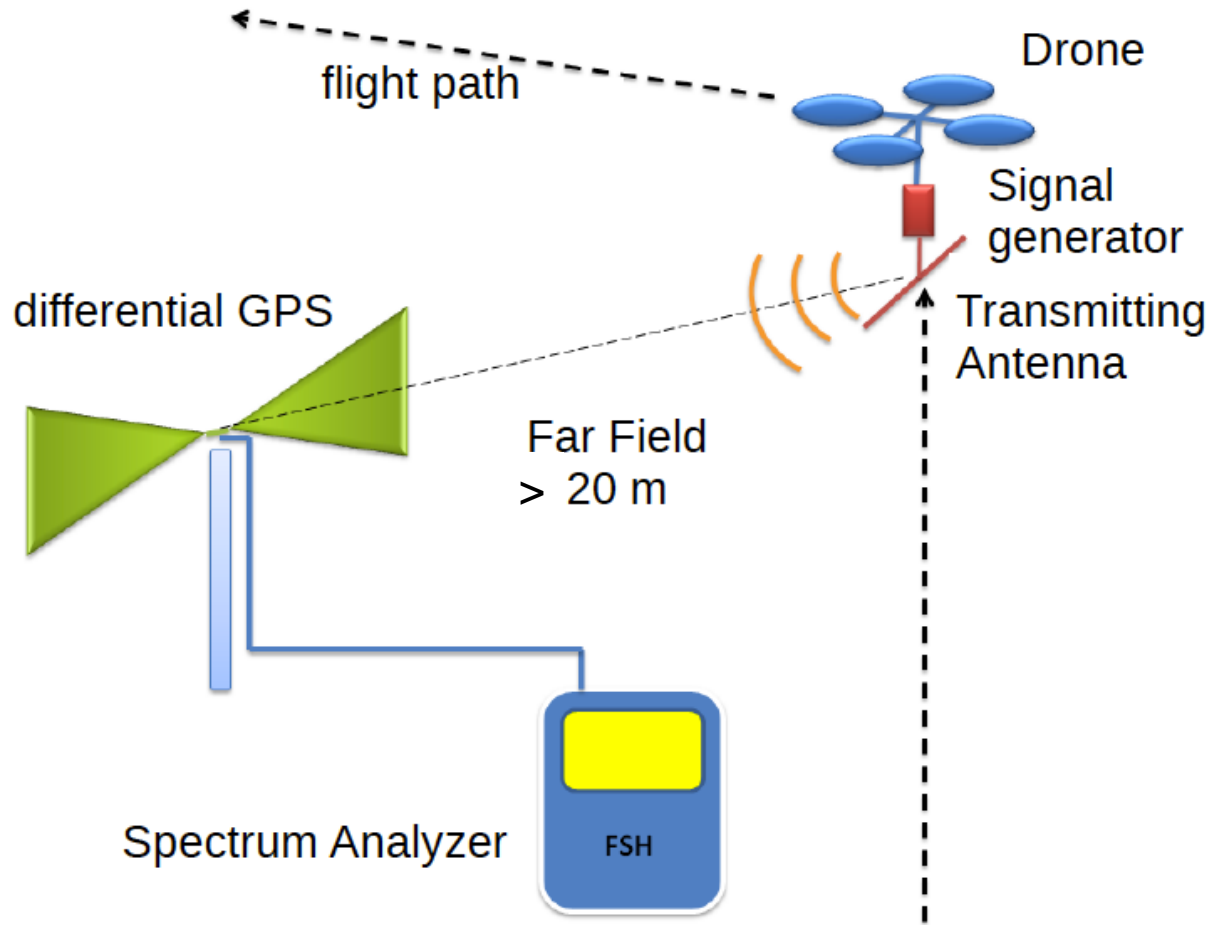
Auger collab. JINST 11 (2016) P01018



**overall time precision
2 ns**

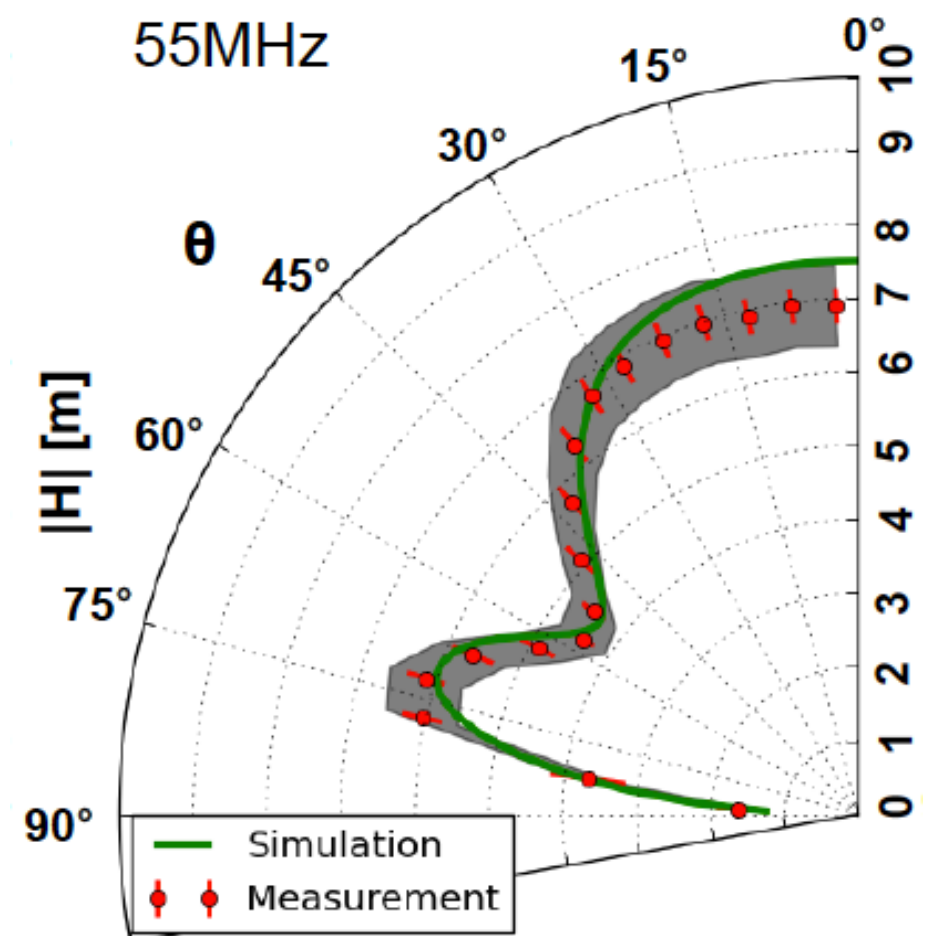
Amplitude calibration

- Direct calibration using a pulser on a drone



vector effective length:

$$V = \vec{H}(f, \theta, \phi) \cdot \vec{E}(f)$$



overall uncertainty: 14% (antenna response + full electronics chain)

Energy measurement

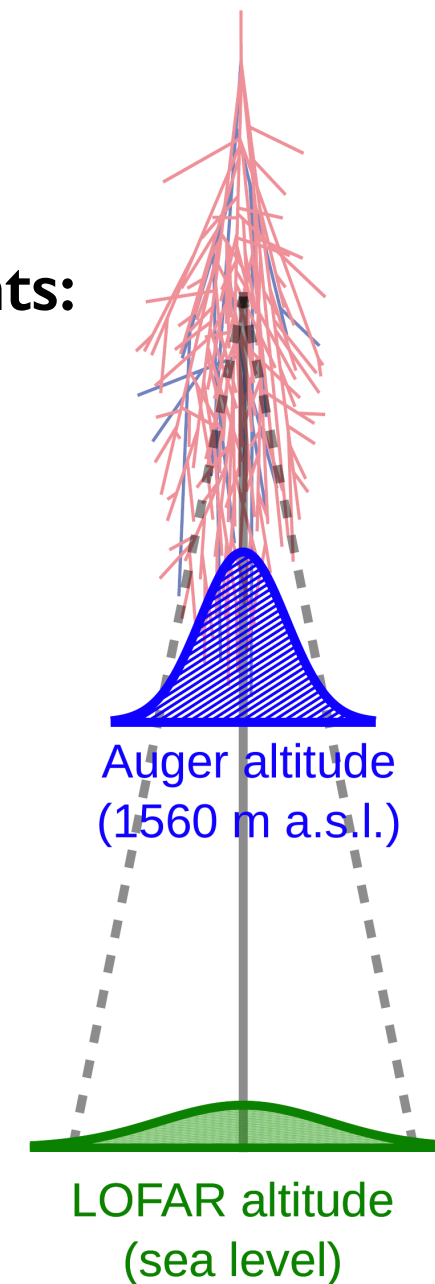
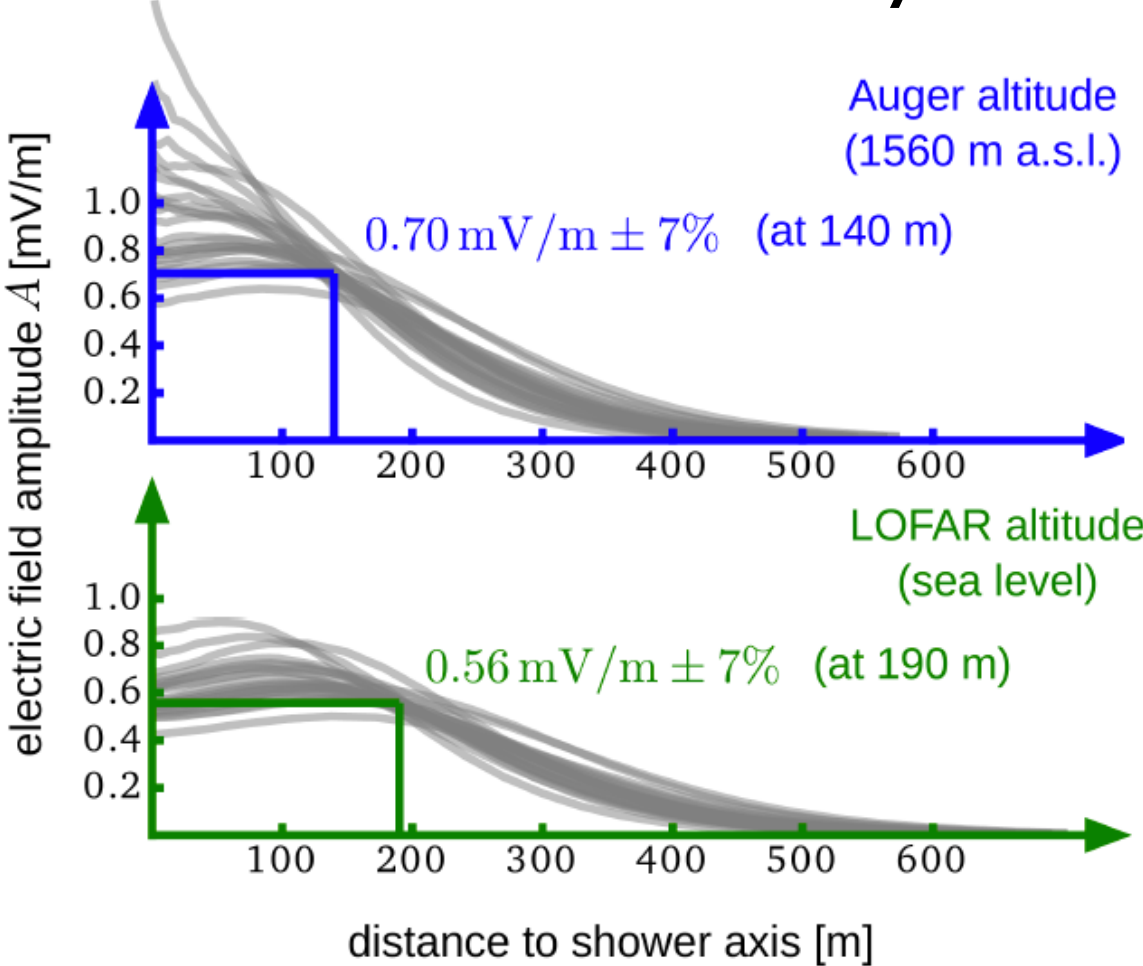
this provides a calorimetric energy estimation from the radiated energy in [30-80] MHz:

$$E_{[30;80] \text{ MHz}} = 15.8 \text{ MeV} \left(\sin \alpha \frac{E}{1 \text{ EeV}} \frac{B}{0.24 \text{ G}} \right)^2$$

Auger collab., PRL 116, 241101 (2016)
Auger collab., PRD 93, 122005 (2016)

- allows to calibrate the detector
- allows to cross-calibrate various CR experiments
- universal method as the atmosphere is transparent to radio waves and first principles based method

one simulated shower seen by two experiments:



two different amplitudes
at two different
optimal axis distances!

but the same
radiated energy:
11.9 MeV